Lithos 202–203 (2014) 167–189

Contents lists available at ScienceDirect

Lithos

journal homepage: www.elsevier.com/locate/lithos

Tracing Neoproterozoic subduction in the Borborema Province (NE-Brazil): Clues from U-Pb geochronology and Sr-Nd-Hf-O isotopes on granitoids and migmatites

Carlos E. Ganade de Araujo [a,b,*], Umberto G. Cordani [b], Roberto F. Weinberg [c], Miguel A.S. Basei [b], Richard Armstrong [d], Kei Sato [b]

[a] Geological Survey of Brazil, Avenida Pasteur 404, CEP 22290-240 Rio de Janeiro, Brazil
[b] Instituto de Geociências, Universidade de São Paulo, Rua do Lago, 562, CEP 05508-080 São Paulo, Brazil
[c] Monash University, School of Geosciences Building 28, Clayton, Melbourne, VIC Australia
[d] Research School of Earth Sciences, Australian National University, Mills Road 0200, Building 142, Canberra, Australia

ARTICLE INFO

Article history:
Received 11 February 2014
Accepted 18 May 2014
Available online 23 May 2014

Keywords:
Neoproterozoic subduction
Water-fluxed melting
Continental collision
West Gondwana Orogen

ABSTRACT

The Ceará Central Domain of the Borborema Province is a key tectonic domain within the 5000 km-long West Gondwana Orogen, which extends from Algeria in Africa to Central Brazil. Igneous rocks of the Tamboril-Santa Quitéria Complex, investigated in this study, record a long-lived history of convergent magmatism and crustal anatexis. SHRIMP U-Pb dating and Hf-O isotope analyses of zircons from granitoids and migmatites, coupled with whole-rock Sr-Nd isotopes were used to constrain the evolution of this long-lived continental margin. Magmatism can be divided into three main periods: i) an early period comprising essentially juvenile arc magmatism at ca. 880–800 Ma and continuing to 650 Ma as evidenced indirectly by detrital zircons from syn-orogenic deposits, ii) a more mature arc period at ca. 660–630 Ma characterized by hybrid mantle–crustal magmatic rocks, and iii) crustal anatexis at 625–618 Ma continuing until ca. 600 Ma. Detrital zircons with mantle values of δO^{18} (<5.7‰) in the range of 950 to 650 Ma retrieved from fore-arc deposits indicate that juvenile input persisted throughout the evolution of the convergent magmatism. Juvenile and mature arc igneous rocks underwent anatexis that gave rise to extensive areas of diatexites within the complex. Anatexis overlap in time with the ages of (ultra)-high pressure (U)HP eclogitic metamorphism dated at 625–615 Ma. In accordance with other continental collision zones, age of UHP/HP metamorphism is interpreted to mark the timing of continental collision and therefore indicate that the anatexis of arc rocks took place during continental subduction in a continent–continent collisional setting. Extensive migmatization continued until ca. 600 Ma and are in part synchronous to the exhumation of the rocks to shallower crustal levels. Thus, the 350 m.y. of magmatic activity in the Ceará Central Domain records the evolution of the West Gondwana margin of the Borborema Province from a juvenile arc setting through a mature arc and continental collision at around 625–600 Ma.

1. Introduction

Subduction zones are sites of intensive magmatism and are currently creating >20% of the terrestrial magmatic products (Tatsumi and Eggins, 1995; Tatsumi, 2005). In these sites, complex compositional variations in magmas arise from interaction between fluids released from the subducting oceanic lithosphere and the overlying mantle wedge, and intrinsic heterogeneities the mantle and magma fractionation (Tatsumi and Kogiso, 2003). Assimilation of crustal material, particularly in Andean-type settings, adds an important component and further variations to the magmas generated in subduction zones (Hildreth and Moorbath, 1988; McMillan et al., 1989).

Subduction of oceanic lithosphere and generation of arcs inevitably precede Himalayan-type collisional orogens. However, in old collisional, deeply eroded terranes, earlier stages of arc magmatism are relatively poorly preserved and have commonly been obliterated by pervasive collisional tectonics. In some extreme cases, earlier arcs can even be subducted along continuous or renewed subduction zones and not be preserved (Yamamoto et al., 2009). Determining at what stage in the tectonic history of a subduction system a magmatic arc begins to evolve from a juvenile state, dominated by mafic-intermediate magmatism, toward a mature state dominated by felsic granitoid plutonism is critical to understand evolution of arcs and the stages preceding continental collision (Treloar et al., 1996). One important fact to consider is whether these earlier arcs are punctual in time, disconnected from the more

* Corresponding author at: Geological Survey of Brazil, Avenida Pasteur 404, CEP 22290-240, Rio de Janeiro, Brazil.
E-mail addresses: caegeo@gmail.com, carlos.ganade@cprm.gov.br (C.E. Ganade de Araujo).

http://dx.doi.org/10.1016/j.lithos.2014.05.015
0024-4937/

mature stage, or are continuously linked to continental arc subduction that precede terminal collision. For example, the Kohistan and Ladakh arcs of northern Pakistan and northwest India represent a Cretaceous early intra-oceanic arc formed during the northward subduction of the Neotethys oceanic lithosphere beneath the Karakoram (e.g. Bard, 1983; Burg et al., 1998; Schaltegger et al., 2002; Weinberg and Dunlap, 2000). This arc was subsequently sutured to the Karakoram Terrane (southern margin of Asia) between 102 Ma and 85–75 Ma (Petterson, 2010). The incorporated arc then became the Andean-type margin (mature stage) of Eurasia until collision with India at around 50 Ma (Hodges, 2000).

Another example is the Mesozoic Sierra Nevada batholith in California, one of the best studied sites for convergent magmatism, where the subduction of the Farallon plate beneath North America during the Triassic to early Cretaceous was characterized by early fringing island arcs just off the Paleozoic continental margin. With continued subduction, a mature stage continental arc was established and a progressively more compressional environment developed as the age of subducting slab continued to young (Busby, 2004; Lee et al., 2007). In this mature arc stage, O-Sr isotopic relations and the variation of $^{147}Sm/^{144}Nd$ with ε_{Nd} suggest that the assimilation of crustal rocks by magmas rising from the mantle and undergoing fractional crystallization could have been the major process responsible for the mixing of crustal- and mantle-derived components (DePaolo, 1981).

In ancient orogenic systems where great part of the petrological history has been obliterated by deformation and/or erosion, zircon can serve as an exceptional crustal growth monitor (Scherer et al., 2007). Coupling of radiogenic and stable isotopes allows measurements of time-stamped hafnium and oxygen isotopes that can uniquely reveal whether zircon crystallized from a mantle-derived source (juvenile) during crustal generation, or from magma derived by reworking of pre-existing igneous or sedimentary rocks (Hawkesworth and Kemp, 2006; Scherer et al., 2007).

In this sense, the Lu-Hf system is analogous to the Sm-Nd, and Hf-Nd isotopes form coherent arrays for most mantle-derived rocks (Vervoort et al., 1999). A larger drawback of relying on Hf isotopes from zircons alone to infer episodes of crustal growth concerns the possibility that the zircons crystallized from magmas with mixed source rocks that separated from the mantle at different times (Hawkesworth and Kemp, 2006). The use of oxygen isotopes greatly reduces this ambiguity, because its fractionation is time-independent. The $^{18}O/^{16}O$ ratio, expressed as $\delta^{18}O$ relative to SMOW, is only changed by low temperature and surficial processes, and so the $\delta^{18}O$ of mantle-derived magmas ($5.7 \pm 0.3‰$) contrasts with those from rocks that have experienced a sedimentary cycle or hydrothermal alteration on the sea-floor, which have elevated $\delta^{18}O$ (Hawkesworth and Kemp, 2006). This is reflected in the high $\delta^{18}O$ of crystallizing zircons and is a fingerprint for a recycled component in granite genesis (Hawkesworth and Kemp, 2006; Hoefs, 2009). Likewise, the Nd-Sr isotopes retrieved from whole-rock analysis also provide a way to make such distinction (DePaolo, 1981; DePaolo et al., 1991; Jacobsen and Pimentel-Klose, 1988) and are useful to monitor and evaluate isotopic differences between data acquired from minerals (e.g. zircon) and rocks from the same representative sample.

The Ceará Central Domain of the Northern Borborema Province, NE-Brazil, was part of a long-lived active continental margin of the West Gondwana Orogen that consumed the Goiás-Pharusian Ocean during the Early Neoproterozoic until final collision at Ediacaran times (Arthaud et al., 2008; Cordani et al., 2013a, 2013b; Fetter et al., 2003; Ganade de Araujo et al., 2012a, 2014). The deep level of exposition, with extensive outcrops of migmatites and exhumed eclogites (Santos et al., 2009), requires the use of isotopic geology to disentangle the evolution of this complex, multi-domain orogenic system. Although timing for arc-building (Andean-type margin) in the Ceará Central Domain is usually attributed to the 650–620 Ma interval (Fetter et al., 2003; Van Schmus et al., 2008), geochronological evidence from detrital zircons in arc-related basins of the Ceará Complex suggests that arc magmatism could have started as early as 900–800 Ma (Ganade de Araujo et al., 2012a). In addition, several occurrences of Early Neoproterozoic juvenile arc assemblages are described along the length of the orogen in Africa and Central Brazil (e.g. Berger et al., 2011; Pimentel and Fuck, 1992). In some cases, these earlier juvenile arcs subsequently evolved into a more mature arc stage preceding final collision that eventually reworked these arcs and precursor basement (continents) during the Late Neoproterozoic (Caby, 2003; Liégeois et al., 1987; Pimentel et al., 2000).

In this study, we focus on the plutonic rocks of the Tamboril-Santa Quitéria Complex in the Ceará Central Domain, that record a long-lived magmatic system attributed to the subduction of the Goiás-Pharusian Ocean during the Neoproterozoic. Here, we combine U-Pb dating and Hf-O isotope composition of zircons, in addition to whole-rock Sr-Nd isotope compositions from granitoids and migmatite protoliths to unravel the tectonic evolution of this complex and their sources (crust vs. mantle) of subduction-related magmas from the Early Neoproterozoic to the final continental collision in the Ediacaran period.

2. Geological setting: the Ceará Central Domain

Excluding the extensional Mesozoic event that separated South America from Africa, the Borborema Province in northeast Brazil is characterized by magmatic, tectonic, and thermal events spanning the Archean to the Cambrian–Ordovician (Brito Neves et al., 2000). The major cratonic blocks involved in the tectonic events that built the Province include (Fig. 1): 1) the Amazonian-São Luiz-West Africa Craton, including the Parnaíba Block; 2) the São Francisco-Congo Craton, and 3) the Paleoproterozoic-Archean collage forming the basement of the Borborema Province (Arthaud et al., 2008; Brito Neves and Cordani, 1991; Brito Neves et al., 2000; Ganade de Araujo et al., 2014; Klein and Moura, 2008). Its final tectonic arrangement was a result of two Neoproterozoic continental collisions: the first and older along the Ceará Central Domain at ca. 620–615 Ma, as part of the West Gondwana Orogen, followed by the collision at ca. 590–570 Ma of the consolidated Borborema Province against the São Francisco Craton along the Sergipano Orogen in the south (Ganade de Araujo et al., 2014; Oliveira et al., 2010).

The Neoproterozoic evolution of West Gondwana Orogen in the Ceará Central Domain results from the development of a convergent margin, related to the consumption of the Goiás-Pharusian Ocean (Cordani et al., 2013a), until the collision between the Parnaíba block (hidden beneath the Phanerozoic Parnaíba basin) and the Paleoproterozoic/Archean basement that extends further east into the Northern Borborema Province (Rio Grande do Norte Domain) (Ganade de Araujo et al., 2014).

The Ceará Central Domain is composed of several litho-tectonic assemblages that include: (1) Archean (ca. 2.8–2.7 Ga) remnants of TTG of the Cruzeta Complex; (2) vast tracts of juvenile Paleoproterozoic (ca. 2.2–2.0 Ga) high-grade amphibolites and felsic to intermediate orthogneisses and migmatites (Fetter et al., 2000; Martins et al., 2009); (3) high-grade Neoproterozoic supracrustal rocks represented essentially by the units of Ceará Complex (e.g. Arthaud, 2007; Arthaud et al., 2008; Ganade de Araujo et al., 2012a); (4) large volumes of Neoproterozoic granitoids represented by the Tamboril-Santa Quitéria granitic–migmatitic Complex (Arthaud et al., 2008; Fetter et al., 2003); and (5) widespread Neoproterozoic to Cambrian post-collisional and Ordovician anorogenic granitoids (Castro et al., 2012). The first two associations are considered as the basement for the Neoproterozoic orogeny.

The Ceará Complex is composed of metamorphosed pelites, semipelites and greywackes, normally showing a prominent schistosity or gneissosity, and is regionally or locally migmatized. Quartzites, marbles, calc-silicate rocks and amphibolites also form large tracts within this complex (Arthaud et al., 2008; Caby and Arthaud, 1986; Cavalcante et al., 2003; Ganade de Araujo et al., 2012a). Taking into account the degree of partial melting, Cavalcante et al. (2003) divided part of the Ceará Complex into the Independência and Canindé units.

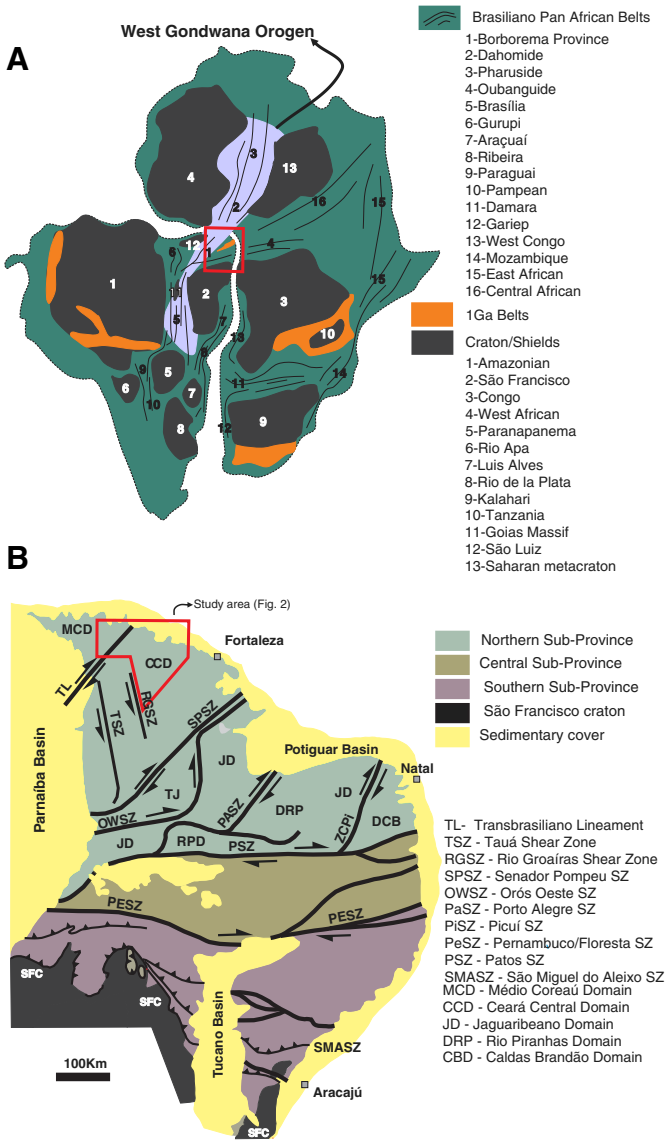

Fig. 1. Main cratonic blocks and mobile belts of the West Gondwana (modified from De Wit et al., 2008) and the Borborema Province and its main sub-divisions.

The supracrustal rocks with only minor migmatization were grouped in the former, whereas those that exhibit significant melting were included in the latter. Locally in the Ceará Complex, felsic sheets and amphibolites interleaved with metasedimentary rocks are interpreted as former volcanic or sub-volcanic rocks and were dated at ca. 800–750 Ma (Arthaud, 2007; Castro, 2004; Fetter, 1999). U-Pb zircon provenance studies from the Ceará Complex demonstrate a heterogeneous provenance pattern characterized by deposits exclusively composed by Paleoproterozoic-Archean detritus, probably representative of small basins floored by sialic crust within the Neoproterozoic orogenic realm, and orogenic arc-related deposits with strong early to middle Neoproterozoic (900–650 Ma) source component (Arthaud, 2007; Ganade de Araujo et al., 2012a).

In the Ceará Complex, retrogressed eclogites have been described to the east and west of the Tamboril-Santa Quitéria Complex. In the east, in the region of Forquilha, retrogressed eclogites occur interleaved with high-grade migmatitic metasedimentary rocks (Ancelmi et al., 2013; Santos et al., 2009) and protolith crystallization was dated at ca. 1.5 Ga (Amaral, 2010). These rocks preserve relics of eclogite facies metamorphism (1.7 GPa, Santos et al., 2009), which may have reached ultra-high pressure (UHP) conditions (Santos et al., 2013) at ca. 615 Ma (Ganade de Araujo et al., in revision). To the west, in the region of Itataia retrogressed eclogites were also described by Castro (2004), however peak pressure conditions (1.4 GPa, Castro, 2004) are lower than those estimated for the Forquilha region.

2.1. The Tamboril-Santa Quitéria Complex

The Neoproterozoic Tamboril-Santa Quitéria Complex (Fig. 2) is a wedge-shaped composite anatectic/igneous association surrounded by metasedimentary rocks of the Ceará Complex. The plutonic rocks display syn- to late-magmatic deformation that was in part coeval with the injection of younger and less deformed magma (Arthaud et al., 2008). In general they range from diorite to granite, with predominance of monzogranitic/granitic rocks (Ganade de Araujo et al., 2012) of the Santa Quitéria unit in its central part.

Previous age determinations indicate that granitoids of this complex range from 640 to 610 Ma (Castro, 2004; Costa et al., 2013; Fetter et al., 2003; Ganade de Araujo et al., 2012; Santos et al., 2007). For this time interval, Nd isotopic signatures are consistent with variable mixtures between juvenile Neoproterozoic magmas and older basement, indicating that the granitoids are hybrid (Fetter et al., 2003). The tectonic setting of this complex has been interpreted as a Neoproterozoic Andean-type magmatic arc (Fetter et al., 2003), however recent works have proposed an evolution from an arc at ca. 850 to 640 Ma into a collisional Himalayan setting (Costa et al., 2013; Ganade de Araujo et al., 2012b).

In the present study the complex is divided into four different units named Lagoa Caíçara, Boi, Santa Quitéria and Tamboril units. Investigated samples from these units and their main features are listed in Table 1.

2.1.1. Lagoa Caíçara unit

This unit comprises a heterogeneous meta-igneous association composed predominantly of stromatic metatexites of granodioritic to tonalitic protoliths (Fig. 3). These meta-igneous rocks are also commonly found preserved as blocks, known as schollen or rafts, within the diatexites of the Tamboril unit. Also in the Lagoa Caíçara unit, sheets of biotite-orthogneisses (c.f. samples DKE-269 and DKE-231) (Fig. 3C and D) with moderate to small volume of leucosomes cut the more complex deformed migmatitic granodiorite–tonalite. Remnants of sedimentary-derived metatexites, of the Ceará Complex are also present within this unit.

Distinction between the different orthogneisses of Lagoa Caíçara unit is difficult in the field. It seems that this unit comprises multiple intrusions of granitoid rocks. Deformation adds complications and it is challenging in many outcrops to ascribe unambiguously a sample to the broader lithological group. In the present study, geochronological and isotopic data permitted the distinction of three different granitoid protoliths in the Lagoa Caíçara unit: i) ca. 880–830 Ma juvenile tonalitic/granodioritic metatexites with high volume of leucosomes, ii) ca. 650 Ma mafic tonalitic metatexites, and iii) ca. 630 Ma crust-derived orthogneisses with low volume of leucosome.

The regional foliation in this unit is simple and has low to moderate dips (<40°) to northwest and north–northwest (Itapajé structural domain in Fig. 2). Along the contact with the diatexites of the Tamboril unit, the stretching lineation has a low rake indicating a strong strike-slip component. They generally plunge gently to ENE and a number of shear sense indicators such as S/C structures suggest a dextral strike-slip movement with a dominant small reverse component. Further south, in the contact between the Lagoa Caiçára unit and the Ceará Complex, the lineation changes to dominantly down-dip, plunging northward and shear sense indicators demonstrate a change to top-to-north-northeast defining normal movement.

The older (830 Ma and 650 Ma) tonalitic to granodioritic protolith of the metatexites contains biotite (10–20%) and hornblende (5–25%) as the main ferro-magnesian phases. The schollen of this unit found

in the Tamboril diatexites have low contents or lack hornblende and are predominantly composed of biotite, plagioclase, K-feldspar and quartz. The neosome of the tonalitic migmatites is composed majorly of plagioclase, quartz and hornblende with no anhydrous peritectic phases, suggesting that melting was due to the influx of water rather than hydrate breakdown reactions (Weinberg and Hasalova, submitted). The younger orthogneisses (ca. 630 Ma) have biotite as the main mafic phase accompanied or not by minor muscovite with K-feldspar invariably more abundant than plagioclase.

2.1.2. Boi unit

The Boi unit differs from the Lagoa Caíçara unit by the presence of more homogenous mafic rocks of predominant quartz-diorite to tonalitic/granodioritic composition (Fig. 5A). They are easily recognizable and mappable in the satellite and gamma-ray image due to characteristic low total counts. In the field these rocks may be strongly foliated to rather isotropic. Migmatitic sectors may occur, however the intrusion of felsic melts may generate pseudo-migmatitic patterns. Rocks from this unit are comprised of plagioclase (45–35%), hornblende (25%-10%), biotite (15–25%), quartz (15–5%) and K-feldspar (8–3%). They are in part intruded by the Santa Quitéria and Tamboril units. Further south of the study area a U-Pb ID-TIMS zircon age of 637 ± 6.5 Ma was obtained for a juvenile ($\varepsilon Nd(600\ Ma) = +3.4$) dioritic migmatitic gneiss (Fetter et al., 2003), possibly associated with the Boi unit.

2.1.3. Santa Quitéria unit

The Santa Quitéria unit forms a large batholith in the central portion of the complex. It is by far the most voluminous magmatic component of the complex and comprises mainly porphyritic K-feldspar monzogranites (Fig. 4B). Composition and strain intensity vary, however toward its central portion, low strain and larger phenocrysts dominate (Fig. 2). Locally, close to the town of Iraúçuba, disrupted rafts of the monzogranite can be found within the diatexite indicating that crustal anatexis occurred after the intrusion of this batholith.

One special feature of this unit is the existence of local disrupted coeval mafic syn-plutonic dykes (Fig. 4D). Geochemical data of these mafic dykes indicate an enriched shoshonitic component derived from mantle sources (Costa et al., 2013; Zincone, 2011). Less common xenoliths of gray orthogneisses, probably derived from the Lagoa Caíçara unit, can also be present within the Santa Quitéria monzogranite. Biotite (20–10%) and hornblende (10–1%) are the main ferro-magnesian phases of Santa Quitéria monzogranites along with plagioclase (40–15%), K-feldspar (35–10%) and quartz (25–15%). Accessories include zircon, titanite, apatite, epidote and opaques. In general, the mafic syn-plutonic dykes are constituted of plagioclase (35–30%), biotite (25–20%), hornblende (20–15%), K-feldspar (15–10%) and quartz (5–2%).

Structurally this unit has a wedge-shaped geometry with foliations in both the NE–SW and E–W trending flanks dipping inwards toward the complex (Fig. 2). In general the regional foliation dips at moderate angles (35–50°) to south–southeast in the northern portion of the domain and to north–northwest in its southern portion (Santa Quitéria structural domain in Fig. 2). The stretching lineation within this domain has low angles and plunges predominantly northeast. Shear sense indicators in the monzogranite indicate top-to-east or northeast sense defining a dominantly strike-slip motion with both normal and reverse components, broadly the same movement direction as defined in the Itapagé domain. This pattern defines the wedge-shaped geometry that some authors attributed as a product of the necking-down of the Tamboril-Santa Quitéria Complex responsible for its extrusion under a transpressive regime as a positive-flower structure (Castro, 2004).

2.1.4. Tamboril unit

The Tamboril unit represents a gradational unit at the contact between the monzogranite of the Santa Quitéria unit and the gneisses and migmatites of the Lagoa Caíçara unit, but generally this unit encircles the Santa Quitéria unit. It is dominated by diatexites containing blocks (rafts or schollen) of both Santa Quitéria porphyritic monzogranite and Lagoa Caíçara orthogneisses. Rafts of Santa Quitéria monzogranites dominate close to the contact with the Santa Quitéria unit whereas high-grade metasedimentary and orthogneisses rafts are found close to the contact of the Lagoa Caíçara unit in the vicinity of Itapajé town.

In general the foliation in these diatexites is defined by a well-developed syn-magmatic flow banding usually defined by biotite schlieren (Fig. 5D). Isotropic domains can be found locally. In the south, along the contact with the Lagoa Caíçara unit, foliation in diatexite dips at moderate angles to NNW with an associated stretching lineation characterized by a strong strike-slip component and shear sense indicators, such as S/C pairs, suggesting a right-lateral movement (top-to-NE). In the north, foliation in the diatexites dips to SSE and E, with a stretching lineation plunging predominantly to SE. Kinematic indicators indicate a top-to-southeast normal displacement; however movement in the opposite direction could also be observed (Fig. 2).

In general, these diatexites lack residual anhydrous peritectic phases, with the exception of rare garnet clusters. Biotite (20–5%) is the main ferro-magnesian phase, but hornblende is present in some samples. In general the rocks tend to have greater concentrations of K-feldspar (45–15%) than plagioclase (25–10%), but in some cases plagioclase can dominate. Previous U-Pb ID-TIMS geochronological data yielded zircon ages for the diatexites of the Tamboril unit in the 620–610 Ma interval (Castro, 2004).

3. Results

Isotopic results and methods for the investigated granitoids and migmatites of the Tamboril-Santa Quitéria Complex are available in the appendix and supplementary data related to this article. Zircon U-Pb, Lu-Hf and oxygen isotopic measurements were all carried out on the same textural domain in each zircon, which permitted us to link age and isotopic parameters directly. A summary of the isotopic data acquired herein is provided in Table 2.

3.1. Zircon SHRIMP U-Pb ages, zircon Hf-O and whole-rock Nd-Sr isotopes

3.1.1. Lagoa Caíçara unit

As described earlier, it is difficult to distinguish the igneous rocks of this unit based solely on their field characteristics. The isotopic results summarized in Table 2 define three groups of igneous rocks based on the age of the protoliths and their sources, which revealed how subduction-related magmas developed through time.

3.1.1.1. Sample DKE-221. This sample is a hornblende-biotite stromatic metatexite of tonalitic composition (Fig. 3A). Zircons were extracted from the paleosome (or the protolith), avoiding contamination with the neosome, and are euhedral, translucent and colorless. In general they range in size from 80 to 200 μm and have length to width ratios ranging from 2:1 to 4:1. Cathodoluminescence images reveal a well-developed oscillatory zoning typical of magmatic zircons (Fig. 6). Some zircons have low-U, thin metamorphic rims, too small for SHRIMP analysis. Analyzed zircons have U contents between 52 and 256 ppm and Th/U ratios ranging from 0.50 to 0.78. Fourteen analyses were done in the zircons and a calculated concordia age using all analyzed zircons yielded an age of 833 ± 6.1 Ma (1σ) (Table 2), interpreted as the crystallization age of the tonalitic protolith (Fig. 7).

Zircons have a significant variation of $^{176}Hf/^{177}Hf$ as a function of $^{206}Pb/^{238}U$ ages with values ranging from 0.282261 to 0.282800 for ages between 880 and 795 Ma. Despite such variations all analyzed zircons yielded consistently positive $\varepsilon Hf_{(t)}$ varying from +0.5 to +19.3 indicating that the tonalitic protolith was derived from mantle or juvenile sources at ca. 830 Ma (Fig. 10A). Oxygen isotopes further support the mantle origin indicated by the Hf isotopes in the zircons. The $\delta^{18}O$ values of 5.09 to 6.24‰ are in agreement with values of mantle

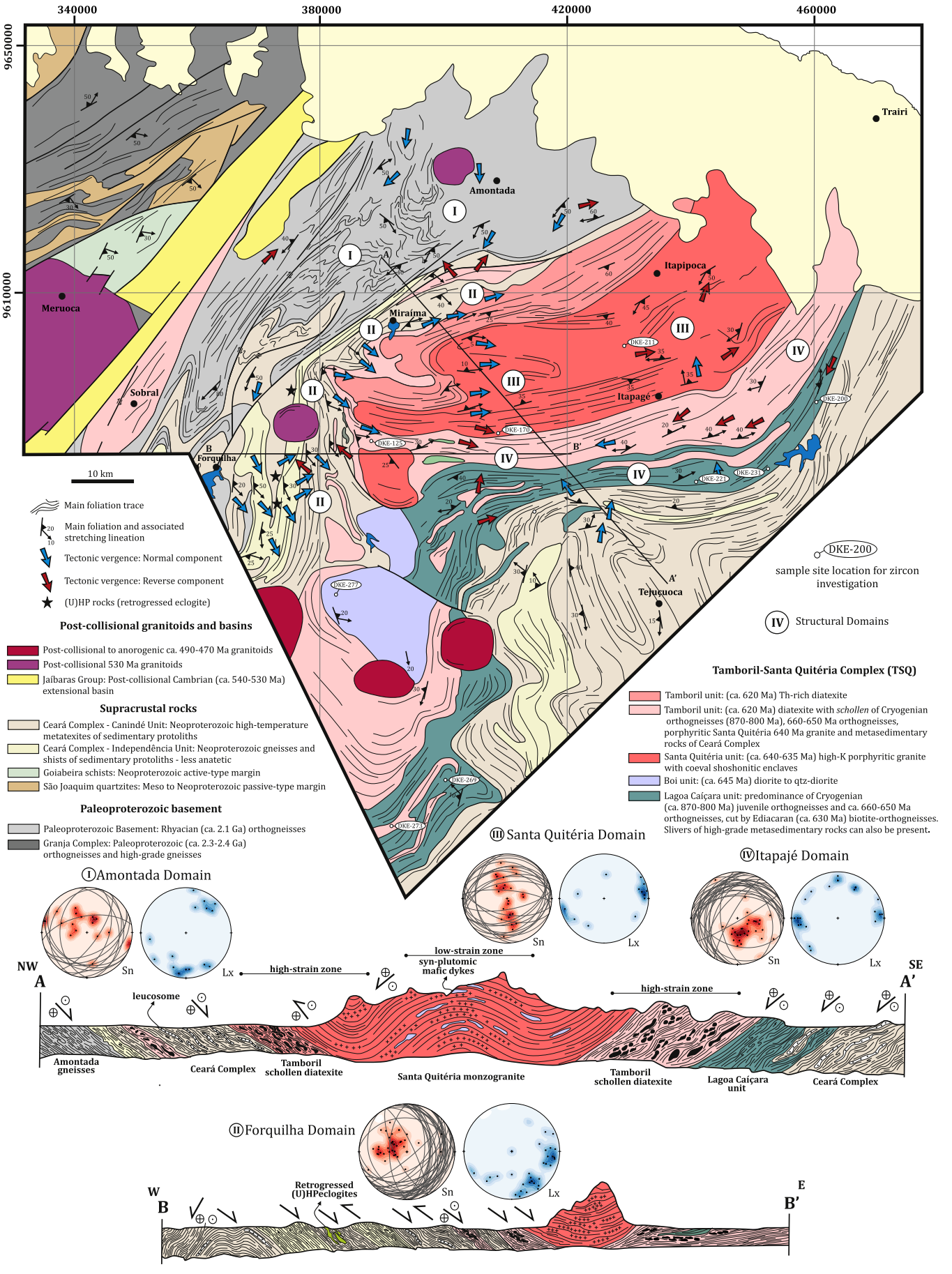

Fig. 2. Geological map and structure of the northern portion of the Tamboril-Santa Quitéria Complex and its neighboring units.

Table 1
Localization and units of the investigated samples from the Tamboril-Santa Quitéria Complex.

Sample	Lithology	Investigated lithology	Unit	UTM
DKE-221	Net-veined granodioritic metatexite	Granodioritic paleosome	Lagoa Caíçara	441417/9577893
DKE-200A	Mafic tonalitic metatexite	Tonalitic paleosome	Lagoa Caíçara	441513/9578525
DKE-269	Gray biotite orthogneisses injected by felsic veins	Orthogneiss	Lagoa Caíçara	406753/9528308
DKE-231	Gray biotite orthogneisses injected by felsic veins	Orthogneiss	Lagoa Caíçara	451924/9581494
DKE-277	Quartz-diorite injected by felsic veins	Quartz-diorite	Boi	381531/9560586
DKE-211	Porphyritic biotite monzogranite	Monzogranite	Santa Quitéria	429040/9601660
DKE-170	Granodioritic metatexite with diatexitic portions	Granodioritic schollen	Tamboril/Santa Quitéria	408537/9587164
DKE-125A	Tonalitic metatexite intruded by felsic granite	Tonalitic paleosome	Tamboril	388123/9585000
DKE-125B	Tonalitic metatexite intruded by felsic granite	Felsic granite	Tamboril	388123/9585000
DKE-273A	Biotite diatexite with granodioritic schollen	Granodioritic schollen	Tamboril	388830/9524195
DKE-273B	Biotite diatexite with granodioritic schollen	Diatexite	Tamboril	388830/9524195

zircon (5.7 ± 0.3‰, Hawkesworth and Kemp, 2006) (Fig. 10B). Whole rock Sr-Nd isotopes also support a juvenile origin for the tonalitic protolith, with low initial $^{87}Sr/^{86}Sr$ of 0.7025 and positive $\varepsilon Nd_{(t)}$ value of +4.98 at the time of crystallization at 833 Ma (Fig. 11).

3.1.1.2. Sample DKE-200A. This mafic tonalitic metatexite was collected in a quarry close to the Itapajé town and differs from the previous sample, not only in age and source, but also by higher content of hornblende (Fig. 3B). Zircons were extracted from the paleosome, avoiding contamination with the neosome. In general they are subhedral to euhedral, translucent and colorless, with dimensions ranging from 60 to 150 μm. They have complex zoned patterns (c.f. zircon #7.1 — Fig. 6) to well-developed oscillatory zoning. Most of the grains have a pronounced metamorphic overgrowth possibly due to the anatexis of the protolith, not dated in this study. Th/U ratios of the dated zircon spots range from 0.55 to 0.85. A concordia age defined by nine concordant zircons yielded an age of 650.6 ± 5.1 Ma (1σ) (Table 2), much younger than the previous sample and interpreted as the crystallization age of the igneous protolith (Fig. 7). $^{176}Hf/^{177}Hf$ ratios from the analyzed zircons vary from 0.282226 to 0.282428 with $\varepsilon Hf_{(t)}$ varying from −3.6 to + 1.5. The $\delta^{18}O$ values for the same zircons in the same CL zones range from 6.73 to 8.19‰ and combined with whole-rock initial $^{87}Sr/^{86}Sr$ ratio of 0.7105 and negative $\varepsilon Nd_{(t)}$ value of −5.45 suggest that this granitoid was predominantly sourced from crustal material, in contrast to the previous sample.

3.1.1.3. Sample DKE-231. This orthogneiss differs from the surrounding migmatitic gneiss found in the same unit by incipient anatexis (e.g. small leucosome volume) absence of hornblende and a more granitic composition (s.l.) than the previous samples (Fig. 3C).

Investigated zircons are colorless and mostly euhedral ranging in size from 80 to 200 μm. They have prominent high-U rim related to

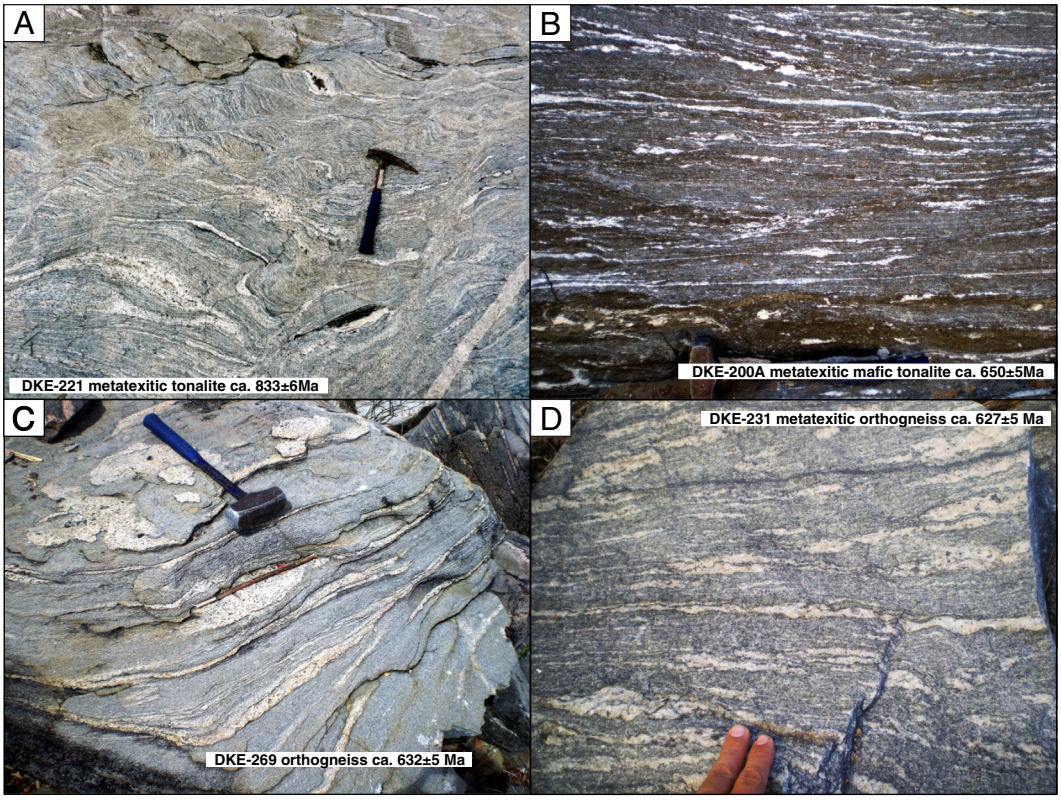

Fig. 3. Field aspects of the studied rocks from the Lagoa Caíçara unit. A. Stromatic metatexite after a 833 ± 6 Ma tonalitic protolith (*sample DKE-221*) with hornblende-bearing leucosomes, interpreted to result from water-fluxed melting. B. Stromatic metatexite after a 650 ± 5 Ma mafic tonalite (*sample DKE-200A*). C. 632 ± 5 Ma biotite gneiss with injected leucocratic veins parallel to the gneissic foliation (*sample DKE-269*). D. Metatexite after a 627 ± 5 biotite orthogneiss (*sample DKE-231*).

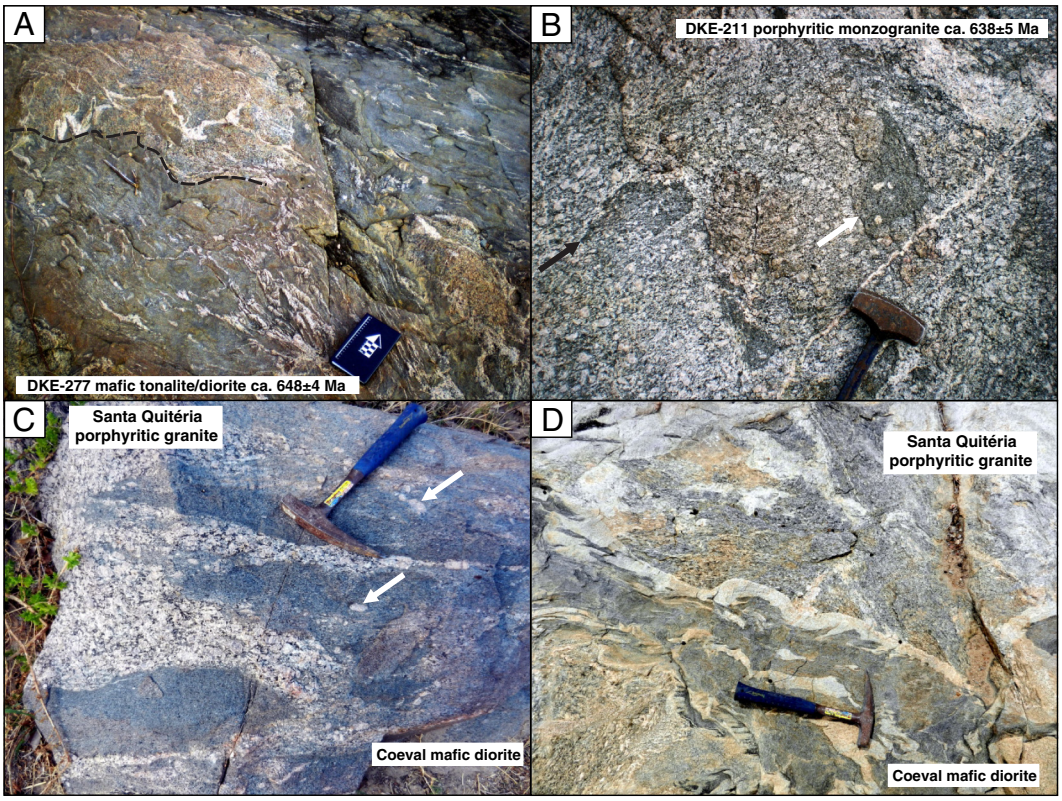

Fig. 4. Field aspects of the studied rocks from the Boi and Santa Quitéria units. A. 648 ± 5 Ma quartz-diorite of the Boi Unit injected by felsic quartz-feldspathic melt (*Sample DKE-277*). B. 638 ± 5 porphyritic monzogranites of the Santa Quitéria unit with mafic enclaves exhibiting crystal-transfer structures (white arrow) (*Sample DKE-211*). C. Coeval Santa Quitéria monzogranite with mafic dioritic enclaves showing evidence for transfer of crystals from the granite to the diorite (arrows). D. Syn-plutonic dykes of diorites cutting through the Santa Quitéria porphyritic monzogranite.

late thermal events (c.f. zircon #6.1 — Fig. 6). Analyzed magmatic zircons have Th/U ratios varying from 0.27 to 0.60 and define a twelve-point concordia age of 627 ± 4.9 Ma (1σ) that reflect the crystallization of the protolith to the orthogneiss (Fig. 7). One zircon with a $^{206}Pb/^{238}U$ age of 691 ± 18 Ma represents an outlier and is likely inherited. No oxygen analysis was carried out for this sample. $^{176}Hf/^{177}Hf$ ratios for the analyzed zircons in spots along the same CL zone range from 0.281848 to 0.282207 with correspondent $\varepsilon Hf_{(t)}$ varying from −18.7 to −6.1, and together with a high initial whole rock $^{87}Sr/^{86}Sr$ ratio of 0.7143 and negative $\varepsilon Nd_{(t)}$ value of −9.65, suggests that this magma was essentially sourced from older crustal rocks.

3.1.1.4. Sample DKE-269. This migmatitic orthogneiss is compositionally similar to the previous one and was found in the same geological context. Zircons from the protolith are euhedral to subhedral with sizes ranging from 50 to 150 μm. Most zircons have a well-developed rim surrounding inherited cores (c.f. zircons #3.1 and #8.1 — Fig. 6). In general Th/U ratios vary from 0.17 to 1.52 (0.17–0.58 for inherited cores). A concordia age of 632 ± 5.1 Ma (1σ) was defined by eleven concordant points and reflects the age of crystallization of the protolith. Three inherited zircons with $^{206}Pb/^{238}U$ ages of 823 ± 23, 796 ± 19 and 761 ± 19 Ma suggest that Early Neoproterozoic protoliths, such as the ca. 830 Ma, juvenile tonalite of sample DKE-221, were involved in the genesis of the protolith. $^{176}Hf/^{177}Hf$ ratios from zircons with $^{206}Pb/^{238}U$ ages in the range of 600 to 658 Ma vary from 0.282323 to 0.282523 with $\varepsilon Hf_{(t)}$ of −1.4 to +5.4, pointing to a juvenile component in the genesis of the precursor magmas. One inherited core yielded a highly radiogenic $^{176}Hf/^{177}Hf$ ratio of 0.282685 with correspondent $\varepsilon Hf_{(t)}$ of +14.5, further supporting the suggestion that juvenile sources were involved in the genesis of the protolith of this orthogneiss. However, $\delta^{18}O$ values range from 8.69 to 10.82‰. This contrasts with expectations from magmas generated by juvenile sources and suggests either crustal material contributed to the formation of the precursor magmas or external, isotopically evolved water was present during melting of the source (see discussion in Section 5.4). High initial $^{87}Sr/^{86}Sr$ ratio of 0.7108 and strong negative $\varepsilon Nd_{(t)}$ value of −10.75 also support the participation of older crustal material in the genesis of the magma.

3.1.2. Boi Unit

3.1.2.1. Sample DKE-277. Zircons from this mafic tonalite are subhedral with ovoid shapes ranging in size from 40 to 100 μm. In general, they have a well-developed igneous oscillatory zoning surrounded by a thin metamorphic overgrowth too thin to be analysed (c.f. zircons 6.1 and 4.1 — Fig. 6). The dated igneous zircons have Th/U ratios of 0.56–0.97 and yielded a twelve-point concordia age of 648 ± 4.1 Ma (1σ) that reflects the age of crystallization of tonalite (Fig. 7). $^{176}Hf/^{177}Hf$ ratios from these zircons have a narrow variation between 0.282201 and 0.282348 which corresponds to $\varepsilon Hf_{(t)}$ values between −6.6 and −0.8. Initial $^{87}Sr/^{86}Sr$ ratio of 0.7056 and negative $\varepsilon Nd_{(t)}$ value of −5.87 indicate that both mantle and older crust were involved in the magma genesis, however $\delta^{18}O$ values for the dated zircons range from 5.48 to 6.25‰, which fall within the proposed range for mantle zircons (5.7 ± 0.3‰, according Hawkesworth and Kemp, 2006).

3.1.3. Santa Quitéria unit

3.1.3.1. Sample DKE-211. This sample of porphyritic monzogranite from the core of the batholith is representative of the most voluminous igneous unit found within the complex. Zircons from this sample (Fig. 4B) are euhedral (80–200 μm) and display nicely developed oscillatory

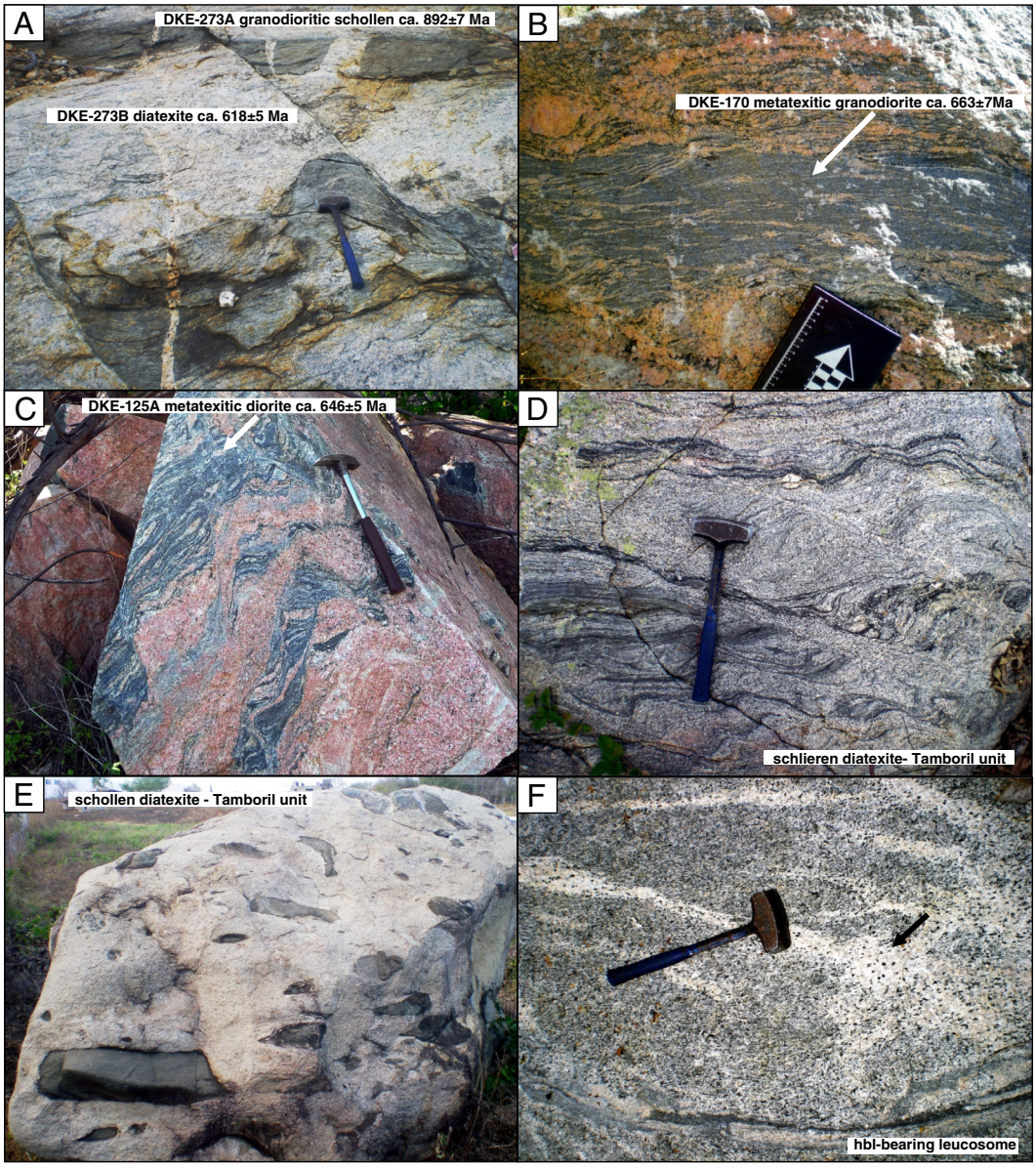

Fig. 5. Field aspects of Tamboril unit. A. Composite outcrop of patchy metatexite after a 882 ± 7 Ma granodioritic orthogneiss (schollen) embedded in a 618 ± 5 granitic diatexite of Tamboril unit within Lagoa Caíçara unit (*Sample DKE-273A and B*). B. Raft of a 663 ± 7 Ma granodioritic orthogneiss embedded in a granitic host close to the contact between Santa Quitéria and Tamboril units (*Sample DKE-170*). C. Folded stromatic metatexite tonalite to diorite (Boi unit) injected by crustal granitic veins of Tamboril unit (*Sample DKE-125*). D. Characteristic flow banding defined by schlieren diatexite of the Tamboril unit. E. Characteristic schollen diatexite of the Tamboril unit. F. Hornblende-bearing leucosomes in diatexite of Tamboril unit.

zoning (Fig. 6) with Th/U ratios ranging from 0.45 to 1.06. Eleven spot analyses yielded a concordia age of 637.8 ± 4.8 Ma (Fig. 7), which reflects the age of crystallization of the monzogranite. This age is slightly younger than the mafic sample DKE-277 from the Boi unit. $^{176}Hf/^{177}Hf$ ratios from the analyzed zircons range from 0.282028 to 0.282314 corresponding to $\varepsilon Hf_{(t)}$ between −12.2 and −2.9, indicating the participation of crustal material in the genesis of the monzogranitic magma, as also suggested by the high $\delta^{18}O$ values of 7.06 to 8.57. Despite the evident interaction with mafic magmas of the Boi unit, high initial $^{87}Sr/^{86}Sr$ ratio of 0.7107 and negative $\varepsilon Nd_{(t)}$ value of −4.25 also point to the involvement of crustal sources in the genesis of this monzogranite.

3.1.4. Tamboril unit

This unit is dominated by granitic diatexites that often contain rafts (schollen) from older igneous rocks of the complex. It represents a gradational unit at the contact between the monzogranite of the Santa Quitéria unit and the gneisses of the Lagoa Caíçara unit and Ceará Complex in the north. The isotopic results do confirm field observations with samples with characteristics similar to those of the Santa Quitéria (DKE-170, DKE-125A) and samples of older juvenile material similar to the Lagoa Caíçara (DKE-273A).

3.1.4.1. Sample DKE-170. Zircons from this metatexitic granodiorite raft (Fig. 5B) from the contact between the Santa Quitéria unit with the diatexites of the Tamboril unit are mostly euhedral (80–150 μm) and characterized by a prominent oscillatory zoning surrounded by a thin high-U metamorphic overgrowth (c.f. zircons 7.1 and 9.1 — Fig. 6). Th/U ratios for the dated zircons vary significantly from 0.11 to 1. Seven concordant analyses fall in a group yielding a concordia age of 663 ± 6.6 Ma (1σ) (Fig. 7). $^{176}Hf/^{177}Hf$ ratios from the analyzed zircons are slightly radiogenic with values ranging from 0.282471 to 0.282741, with correspondent $\varepsilon Hf_{(t)}$ of +3.7 to +13.2, indicating the

Table 2
Summary of the main isotopic features of the investigated samples.

Sample	Lithology	Unit	Age (Ma)	Inheritance (Ma)	εHf(t)zircon	(Source)	δ^{18}Ozircon (‰)	(Source)	εNd(t)	(Source)	($^{87}Sr/^{86}Sr$)	(Source)
DKE-221	Granodioritic metatexite (protolith)	Lagoa Caiçara	833 ± 6.1	No	(+0.5 to +19.3)	Mantle	(5.09 to 6.24)	Mantle	(+4.98)	Mantle	(0.7025)	Mantle
DKE-200A	Mafic tonalitic metatexite (protolith)	Lagoa Caiçara	654.6 ± 4.7	No	(−3.6 to + 1.5)	Mantle/crustal	(6.73 to 8.19)	Mantle	(−5.45)	Crustal	(0.7105)	Crustal
DKE-269	Gray biotite orthogneiss	Lagoa Caiçara	632 ± 5.1	820–761	(−1.4 to +5.4)	Mantle/crustal	(8.69 to 10.82)	Crustal	(−10.75)	Crustal	(0.7108)	Crustal
DKE-231	Gray biotite orthogneiss	Lagoa Caiçara	627 ± 4.9	No	(−18.7 to −6.1)	n.a.	n.a.	n.a.	(−9.65)	Crustal	(0.7143)	Crustal
DKE-277	Quartz diorite	Boi	648 ± 4.1	No	(−6.6 to −0.8)	Crustal	(5.48–6.25)	Mantle	(−5.87)	Crustal	(0.7056)	Crustal/mantle
DKE-211	Porphyritic monzogranite	Santa Quitéria	637.8 ± 4.8	No	(−12.2 to −2.9)	Crustal	(7.06 to 8.57)	Crustal	(−4.25)	Crustal	(0.7107)	Crustal
DKE-170	Granodioritic schollen	Tamboril/Santa Quitéria	663 ± 6.6	No	(+3.7 to +13.2)	Mantle	(5.94–9.06)	Crustal	(+1.80)	Mantle	(0.7028)	Mantle
DKE-125A	Tonalitic metatexite (protolith)	Tamboril	646 ± 4.5	No	n.a	n.a.	n.a.	n.a.	n.a.	n.a.	n.a.	n.a.
DKE-125B	Tonalitic metatexite (schollen)	Tamboril	625.9 ± 4.6	No	n.a	n.a.	n.a.	n.a.	n.a.	n.a.	n.a.	n.a.
DKE-273A	Granodioritic metatexite (schollen)	Tamboril	892 ± 7.5	No	(−3.6 to + 1.5)	Mantle/crustal	(5.20 to 6.44)	Mantle	(+3.84)	Mantle	(0.7020)	Mantle
DKE-273B	Diatexite matrix	Tamboril	618 ± 4.1	879–728	(−1.4 to + 5.4)	Mantle/crustal	(6.41 to 9.10)	Mantle	(−3.55)	Crustal	(0.7079)	Crustal

involvement of juvenile sources in the genesis of the magmas. Low initial $^{87}Sr/^{86}Sr$ ratio of 0.7028 and positive $\varepsilon Nd_{(t)}$ value of +1.80 also lend support to partial melting of depleted mantle sources. However, the $\delta^{18}O$ values (5.94–9.06‰) for the dated igneous zircons fall outside the field of mantle zircons and suggest that crustal contaminants or isotopically evolved water interaction during crystallization could contribute to the observed higher $\delta^{18}O$ values.

3.1.4.2. Sample DKE-125. We collected two samples in this outcrop. Sample DKE-125A is a mafic stromatic metatexitic diorite raft embedded in the granitic diatexite of the Tamboril unit. Sample DKE-125B represents the host granite diatexite (Fig. 5C). Field evidence does not support the derivation of the diatexite from the partial melting of the diorite because the leucosomes in the diorite have different composition to the host diatexite evidenced by abundant plagioclase. Zircons from the metatexitic diorite are euhedral to subhedral (60–200 μm) and have well-defined igneous oscillatory zoning with Th/U ratios ranging from 0.50 to 0.80. Twelve zircons form a group in the concordia line yielding a mean age of 646 ± 4.5 Ma (1σ) for the dioritic protolith crystallization (Fig. 7). Zircons from the host granitic diatexite are also euhedral to subhedral and have well-defined igneous oscillatory zoning with Th/U ratios from 0.13 to 0.84. A concordia age of 625.9 ± 4.6 Ma (1σ) defined by eleven concordant analyses reflects the age of the crystallization of this diatexite (Fig. 7). No zircon Hf-O isotopes or whole-rock Sr-Nd analyses were performed for either of these samples. These results suggest that mafic intrusive rocks of an age similar to that of the Boi unit were involved in an anatectic event that occurred only 20 m.y. after their crystallization.

3.1.4.3. Sample DKE-273. The composite sample DKE-273 is divided into a schollen of granodioritic composition (sample DKE-273A) and the host diatexite of the Tamboril unit (sample DKE-273B) (Fig. 5A). Different from sample DKE125, field evidence such as continuity between the host diatexite and leucosomes in the schollen, as well as textural similarity supports partial melting of the granodioritic schollen as one of the sources of the diatexite. Zircons from the granodioritic schollen are euhedral, transparent, and colorless to light yellow. Most of them are equant to short prismatic. Crystals range in length from 80 to 200 μm. Most zircons are oscillatory zoned and interpreted as the result of magmatic growth (c.f. zircons 16.1 and 15.1 — Fig. 6), but newly developed rims around magmatic cores also with a characteristic oscillatory zoning are interpreted as melt-precipitated zircons from the partial melting event (c.f. zircons 5.2 and 7.1 — Fig. 6). A third type of zircon is characterized by homogenous domains that crosscut the two types described above (c.f. zircon 12.2 — Fig. 6). Two clusters of crystallization ages were obtained from zircons in the schollen. The older, with a calculated concordia age of 892 ± 7.5 Ma is considered to be the protolith age, and was obtained from both old cores (c.f. zircons 5.2 and 7.1 — Fig. 6) and from zircons with prominent oscillatory zoning but lacking overgrowths (c.f. zircons 16.1 and 15.1 — Fig. 6). The younger cluster with a calculated concordia age of 620 ± 5.1 Ma (Fig. 7) is interpreted as the age of anatexis and was obtained from magmatic overgrowths (melt-precipitated) around older cores (c.f. zircons 5.2 and 7.1 — Fig. 6). We note that this age is similar within error to the age of the anatectic matrix of the previous sample DKE125B. Th/U ratios in this sample vary systematically with younger zircons showing lower ratios (0.07–0.22) while the older zircons demonstrate higher values (0.22–0.67).

The analyzed zircons for sample DKE-273A zircons have Initial $^{176}Hf/^{177}Hf$ ratio with values ranging from 0.282104 to 0.282249 for ages between 904 and 846 Ma and correspondent $\varepsilon Hf_{(t)}$ varying from −3.6 to + 1.5. The highest $(^{176}Hf/^{177}Hf)_i$ ratio of 0.282348 occurs in an inherited zircon with a $^{206}Pb/^{238}U$ age of 959 Ma, corresponding to the maximum $\varepsilon Hf_{(t)}$ value of +6.2. Two grains with well-defined younger melt-precipitated rims were analyzed with $^{206}Pb/^{238}U$ ages of 638 and 622 Ma and correspondent $\varepsilon Hf_{(t)}$ of −0.9 and +0.1, respectively.

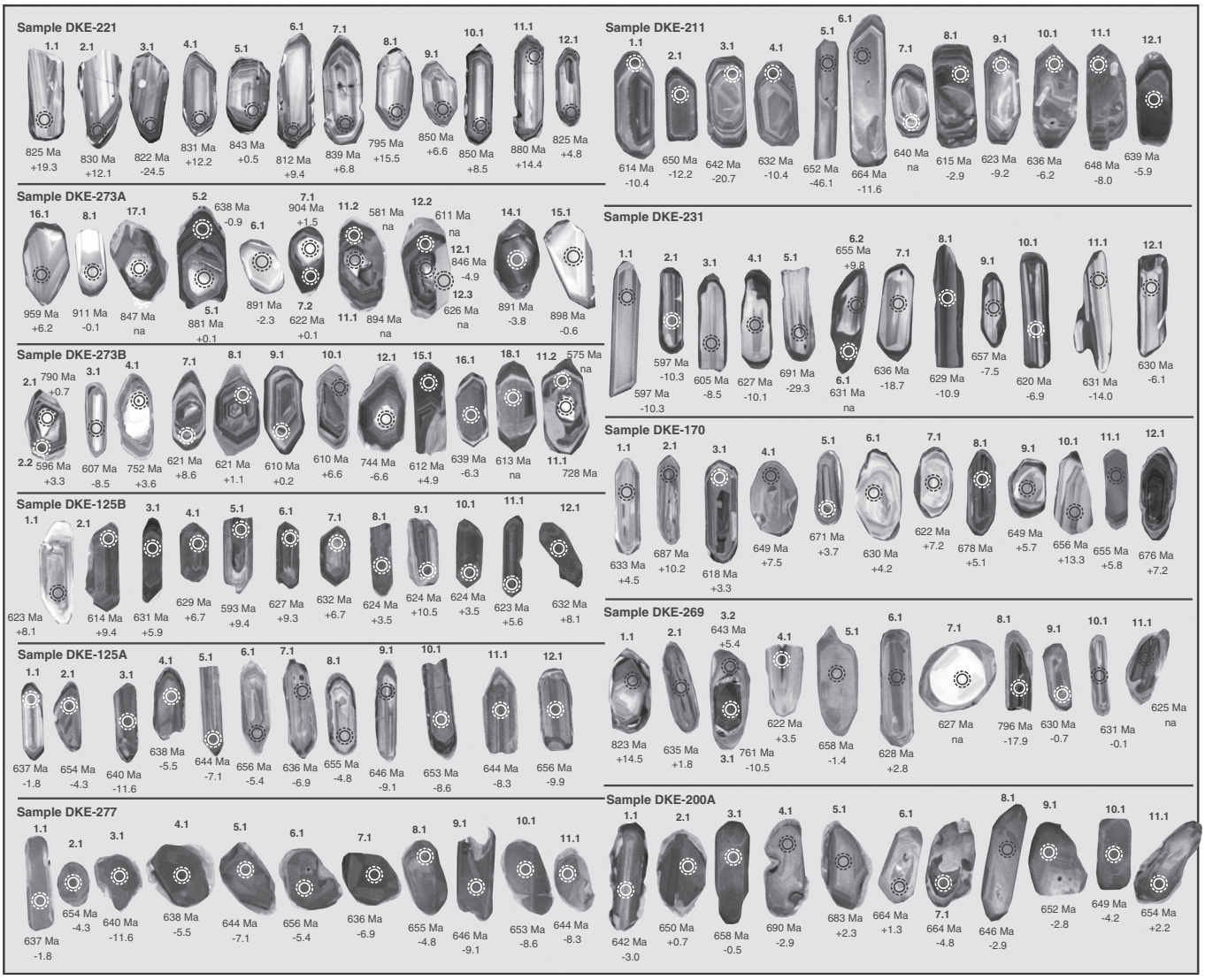

Fig. 6. Cathodoluminescence images from zircons selected for U-Pb geochronology and Hf-O isotopic investigation.

Although the $\varepsilon Hf_{(t)}$ for the zircons of the granodioritic protolith yielded mostly neutral values hampering the possibility of evaluation between the distinction of juvenile and crustal material, time-resolved oxygen isotopes on the same zircons were more conclusive. The $\delta^{18}O$ values for the older zircons (830–959 Ma) of 5.20 to 6.44‰ fall mostly within the range of mantle zircon (5.7 ± 0.3‰), indicating the addition of juvenile mantle-derived material in the referred time. Conversely, $\delta^{18}O$ values of 7.69 to 8.17‰ for the melt-precipitated rims (643–581 Ma) are significantly higher than the mantle zircon, indicating involvement with crustal material or addition of water during the melting event. The granodioritic schollen also have low initial $^{87}Sr/^{86}Sr$ of 0.7020 and positive $\varepsilon Nd_{(t)}$ of +3.84 at (t = 892 Ma), pointing to the derivation of juvenile mantle-derived sources.

Sample DKE-273B, representative of the diatexite matrix yielded younger ages and several inherited zircons from the melted protolith. Zircons from this sample are also euhedral, transparent, colorless, with crystals ranging in length from 80 to 200 μm (Fig. 6). The calculated concordia age at 618 ± 4.1 Ma (Fig. 7) was acquired from newly formed zircons from the melt (c.f. zircons 3.1 and 9.1 — Fig. 6) or from melt-precipitated overgrowths around older magmatic cores (c.f. zircons 2.2 and 7.1 — Fig. 6). This age is equivalent to that obtained from the melt-precipitated overgrowths found in the zircons from the schollen in sample DKE-273A and also from the diatexite sample DKE125B, and represents more precisely the time of the anatexis. Ages from older cores (c.f. zircons 2.1 and 4.1 — Fig. 6) scatter between 728 and 879 Ma and do not define a precise age in the concordia diagram, suggesting an inherited nature from the precursor source material prior the melting event. In general, variations between the initial $^{176}Hf/^{177}Hf$ ratio and the $^{206}Pb/^{238}U$ ages for the melt-precipitated zircons in diatexite of the sample 273B are significantly higher than the zircons extracted from the schollen, with values ranging from 0.282152 to 0.282687 for ages between 637 and 607 Ma and correspondent $\varepsilon Hf_{(t)}$ varying from −1.4 to + 5.4 (Fig. 10A). Two older cores, inherited from the schollen were also analyzed and yielded $\varepsilon Hf_{(t)}$ of −0.5 and +14.5, suggesting some incorporation of juvenile material from the schollen protolith, as expected from field observations. The $\delta^{18}O$ values for the melt-precipitated rims and newly formed zircons of 6.41 to 9.10‰ are also higher than the mantle zircon, indicating the addition of water during the melting event and or contamination with crustal material (Fig. 10B). As also expected, the older cores inherited from the schollen have mantle signatures with zircons values ranging from 4.64 to 5.53‰ (Fig. 10B). This diatexite has initial $^{87}Sr/^{86}Sr$ ratio of 0.7079 and negative $\varepsilon Nd_{(t)}$ of −3.55 at t = 618 Ma, suggesting that crustal material was also involved in the genesis of the diatexites (Fig. 11).

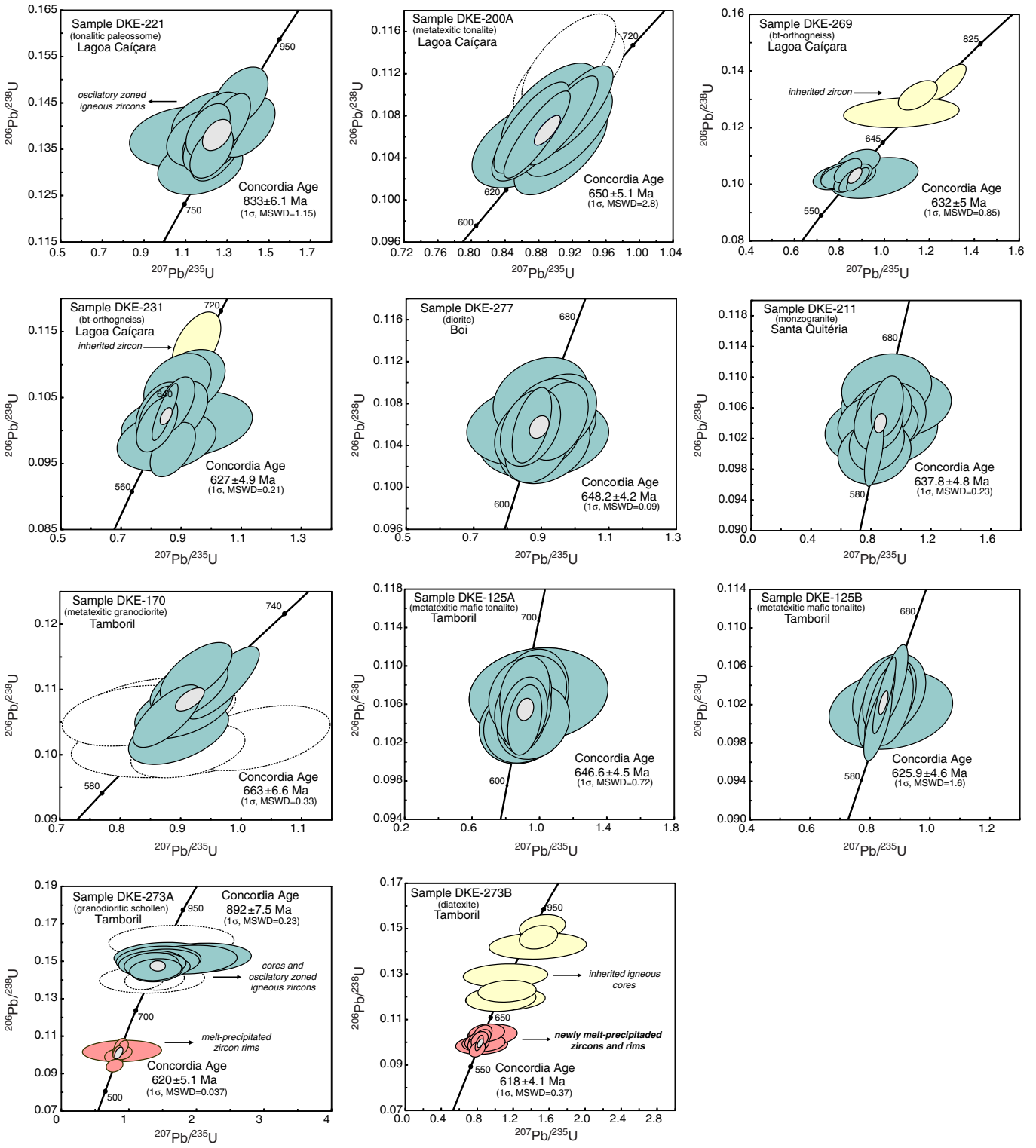

Fig. 7. U-Pb Whetheril concordia diagrams for the investigated samples. Green elipses indicate protolith crystallization; yellow ellipses indicate inheritance; pink ellipses indicate melt precipitated zircons; white ellipses were excluded from the dataset. (For interpretation of the references to color in this figure legend, the reader is referred to the web version of this article.)

3.2. Zircon SHRIMP O isotopes in detrital zircons

Forty-one analyses of Neoproterozoic zircons (939–648 Ma) extracted from two samples of metatexitic paragneisses (samples DKE-43 and 45) of the Ceará Complex (close to Miraíma town) were also performed to evaluate the changes in mantle and crustal involvement with time. $^{206}Pb/^{238}U$ ages of the same analyzed zircons were previously acquired by Ganade de Araujo et al. (2012a) and the ages of the paragneisses are younger than 650 Ma and their anatexis was estimated to be at 640–600 Ma.

According to these authors zircons were shed from a long-lived arc system (the Tamboril-Santa Quitéria Complex) and deposited in a forearc basin. In general both samples have a significant variation between low and high $\delta^{18}O$ values, however, lower mantle-like values ($\delta^{18}O < 6.0‰$) are consistently more abundant in the sample DKE-43. The $\delta^{18}O$ values for this sample range from 3.64 to 8.11‰ with 78% of the total analyzed zircons (n = 22) exhibiting values of $\delta^{18}O < 6.0‰$ throughout the range of 949 to 648 Ma (Fig. 10B). For the sample DKE-45 $\delta^{18}O$ values vary from 5.09 to 7.73‰ with 36% of the analyzed zircons (n = 19) showing values <6.0‰ for a narrower range of time between 932 and 711 Ma (Fig. 10B). $^{206}Pb/^{238}U$ ages and $\delta^{18}O$ values indicate that mantle derived sources persisted throughout time since the beginning of the Neoproterozoic arc magmatism, however the presence of zircons with high $\delta^{18}O$ values (>6.0‰) from 869 to 662 Ma also suggests that the sources (magmas) of these zircons also have interacted with crustal materials.

3.3. Major and trace elements

Geochemical results do not allow discrimination among the major units of the Tamboril-Santa Quitéria Complex, instead, granitoids show similar trace and REE patterns mostly characteristic of convergent plate margins.

3.3.1. Lagoa Caiçara unit

The non-melted portions of the older group of gneisses and migmatites (ca. 830 Ma) have SiO_2 ranging from 65.3 to 68.2 wt.%. The K_2O contents range between 2.1 and 5.9 wt.% with an average of 3.9 wt.% with the samples plotting mostly in the high-K calc-alkaline field in the K_2O versus SiO_2 classification diagram of Peccerillo and Taylor (1976) (Fig. 8A). Their Al_2O_3 contents range from 13.8 to 19.6 wt.% yielding a metaluminous to subordinately weak peraluminous signatures (ASI = 0.73–1.08) (Fig. 8B). The geochronological data presented herein identified not only Early Neoproterozoic migmatitic orthogneisses, but also orthogneisses, whose protoliths have crystalized at ca. 650 Ma. These ca. 650 Ma orthogneisses have SiO_2 ranging from 55.5 to 62.2 wt.% with an average of 57.7 wt.% and similar K_2O (1.77–4.86 wt.%) contents of the older gneisses.

In the primitive mantle-normalized spidergram (Fig. 9), the samples from both groups (ca. 800 and ca. 650 Ma) show characteristic negative anomalies of Th, Nb, La, P and Ti. In the case of P and Ti this is attributed to a residue of apatite and ilmenite in the parental magma. These rocks have similar REE contents when compared with typical I-type granites. All samples of the older group (ca. 800 Ma) exhibit high REE contents, relatively enrichment of LREE ((La/Yb)N ratios of 4.3 to 44.5 with an average of 10.2), flat HREE patterns ((Tb/Yb)N ratios of 1.0 to 2.4) and strong to weakly negative Eu anomalies (Eu/Eu^* ratios of 0.56 to 0.99) (Fig. 9). Samples from both groups plot within the VAG field in the tectonic discriminant diagram of Pearce et al. (1984) and in the active-margin granites of Schandl and Gorton (2002) (Fig. 8C and D).

3.3.2. Boi unit

In general, samples from this unit have SiO_2 ranging from 67.0 to 69.1 wt.% with an average of 67.8 wt.%. They have rather high K_2O (2.4–7.4 wt.%) and low MgO (0.63–1.0 wt.%) contents with samples plotting mostly in the high-K calc-alkaline field in the K_2O versus SiO_2 diagram (Fig. 8A). Their Al_2O_3 contents are between 14.9 and 15.7 wt.% giving the rock a weak peraluminous signature (ASI = 0.99–1.06) (Fig. 8B). They have low Ba (479–868 ppm) and Sr (152–329 ppm) contents, and characteristic negative anomalies of Nb and Ti and positive anomalies of U, K and Ce in the primitive mantle-normalized spidergram (Fig. 9). Normally, the samples show a relatively enrichment of light rare earth elements (LREEs)($(La/Yb)_N$ ratios of 8.2 to 91.5 with an average of 11.8), and a predominant strong negative Eu anomalies (Eu/Eu^* ratios ≈ 0.63).

3.3.3. Santa Quitéria unit

Geochemically, the samples of Santa Quitéria unit have SiO_2 contents in between 58.7 and 75.4 wt.%, with an average of 61.1 wt.%. K_2O contents range between 1.8 and 7.4 wt.% with an average of 3.1 wt.% with the samples plotting mostly in the high-K calc-alkaline and shoshonitic fields in the K_2O versus SiO_2 classification diagram of Peccerillo and Taylor (1976) (Fig. 8A). The samples demonstrate overall patterns of decreasing Mg, Fe, Ca, Ti, Al and P with increasing SiO_2. Their Al_2O_3 contents are in between 13.3 and 17.4 wt.% indicating a metaluminous to weak peraluminous character (ASI = 0.73–1.07) (Fig. 8B). The samples display an enriched LILE pattern, defining a downward sloping profile in the primordial mantle normalized spidergram, combined with positive anomalies of K, Pb and Nd and negative Nb, Th, P and Ti anomalies (Fig. 9). In spite of the significant variance of Ba and Sr, the former appears especially abundant, with average values of 727 and 223 ppm, respectively. Generally the analyzed samples exhibit high REE contents, relatively enrichment of light rare earth elements (LREEs)($(La/Yb)_N$ ratios of 3.3 to 67.8 with an average of 14.9), flat HREE patterns ($(Tb/Yb)_N$ ratios of 0.7 to 3.1) and predominant negative Eu anomalies (Eu/Eu^* ratios ≈ 0.83).

3.3.4. Tamboril unit

In general terms, samples of the Tamboril diatexite are geochemically similar to those of the Santa Quitéria unit. They have SiO_2 ranging from 62.4 to 68.3 wt.% with an average of 64.3 wt.%. K_2O contents range between 1.6 and 6.5 wt.% with an average of 3.9 wt.% with the samples plotting mostly in the high-K calc-alkaline and shoshonitic fields (Fig. 8A). Their Al_2O_3 contents are in between 13.6 and 16.9 wt.% that gives a metaluminous to subordinately weak peraluminous characteristic (ASI = 0.84–1.04) (Fig. 8B). In the primitive mantle-normalized spidergram samples show characteristic negative anomalies of Nb, P and Ti that should be attributed in part to residue of apatite and ilmenite in the parental magma. The samples exhibit high REE contents, relative enrichment of light rare earth elements (LREEs)($(La/Yb)_N$ ratios of 2.9 to 85.1 with an average of 20.4), flat HREE patterns ($(Tb/Yb)_N$ ratios of 0.7 to 4.7) and predominant negative Eu anomalies (Eu/Eu^* ratios ≈ 0.63) (Fig. 9).

4. Discussion

4.1. Magmatic evolution

Geochemistry, U-Pb zircon ages, time-resolved zircon Hf-O isotopic determinations and whole-rock Sr-Nd isotopes of the Tamboril-Santa Quitéria Complex provide important constraints on the magmatic and tectonic evolution of the Ceará Central Domain. Trace element concentrations of the investigated samples display a typical spectrum of arc-related igneous rocks, the so-called “arc-signature”, characterized by the enrichment of highly mobile large ion lithophile elements (LILE) relative to high field strength elements (HFSE) (McMillan et al., 1989). However, it is the isotopic composition that characterizes better the source of the investigated granitoids. Essentially, magmatism can be divided into three main periods with their particular characteristics: i) an early period comprising essentially juvenile arc magmatism at ca. 880–800 Ma, ii) a more mature arc period at ca. 660–630 Ma characterized by hybrid mantle–crustal components, and iii) crustal anatexis at 625–618 Ma continuing until ca. 600 Ma. In the following discussion we will avoid the unit nomenclature based on mapping, and divide the investigated samples according to their age and isotopic signatures.

4.1.1. Early 880–800 Ma juvenile arc-related magmatism

Samples 273A and DKE-221 of granodioritic/tonalitic composition, yielded the oldest zircon crystallization ages at 892 ± 7.5 and 833 ± 6.1 Ma, respectively. These samples have predominantly positive $\varepsilon Hf_{(t)}$ (−3.6 to + 19.3) and positive $\varepsilon Nd_{(t)}$ (+4.98 to +3.84)

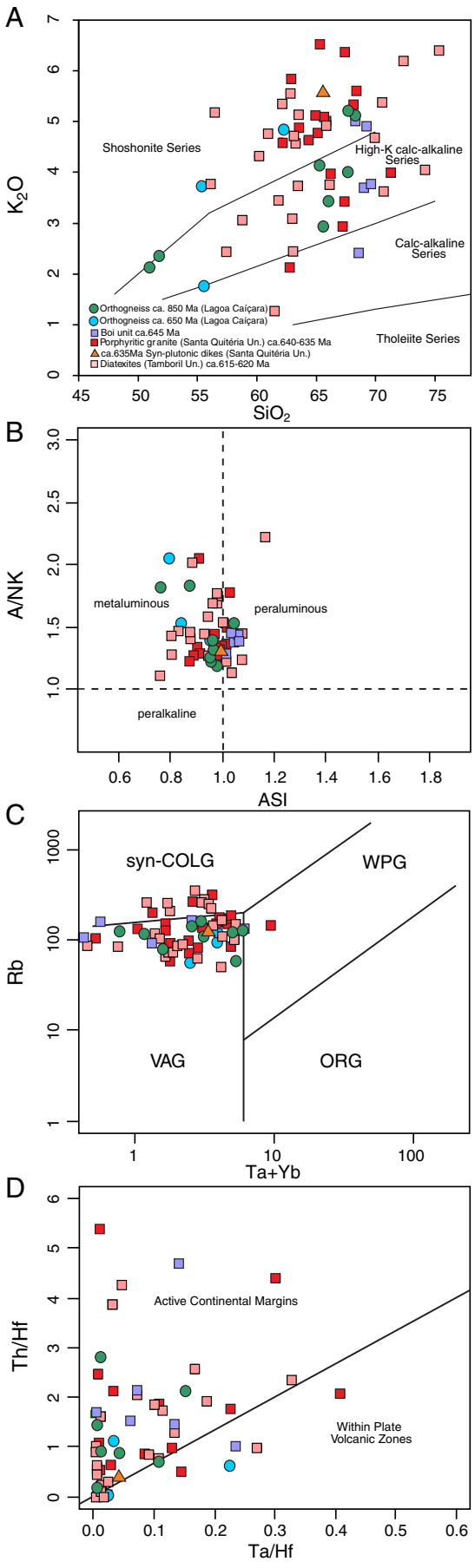

combined with low initial $^{87}Sr/^{86}Sr$ (<0.7025), suggesting derivation from a depleted mantle (juvenile) source. Detrital zircons from forearc deposits of the Ceará Complex suggest that magmatism was continuously active from at least ca. 900 to ca. 650 Ma (Ganade de Araujo et al., 2012a) (Fig. 12). The $\delta^{18}O$ values retrieved from the same detrital zircons previously dated by these authors (samples DKE-43 and DKE-45 of the Ceará Complex), indicate that the juvenile input persisted throughout great part of the convergent magmatism ascribed to the consumption of the Goiás-Pharusian Ocean (Fig. 10B).

Geochemistry of these 880–800 Ma tonalitic to granodioritic rocks suggests that this juvenile signature was acquired in an arc-related setting rather than during rifting. In the Ceará Central Domain, some authors favor break-up and rift development at around 770–750 Ma (Arthaud, 2007; Brito Neves and Fuck, 2013; Castro, 2004; Fetter et al., 2003), however the lack of characteristic features of rift settings such as concomitant immature terrigenous sedimentation, abrupt tectonically-controlled facies variations and abundant bimodal volcanism, does not support this idea. Instead, such extensional event may be related to an extensional subduction setting and development of diachronous back-arc basins to the east of the Lagoa Caíçara unit. On the other hand, a U-Pb ID-TIMS age of ca. 770 (Fetter et al., 2003) retrieved from volcanic rocks found associated with passive margin deposits of the Martinópole Group in the Médio Coreaú Domain (west of the Transbrasiliano Lineament in Fig. 2) suggests that extension and passive margin development was concurrent with subduction and arc development in the Ceará Central Domain.

Evidence from the West Gondwana Orogen in Africa (Berger et al., 2011; Caby, 1989, 2003; Dostal et al., 1994) and Central Brazil (Laux et al., 2005; Pimentel and Fuck, 1992; Pimentel et al., 2000) demonstrates that part of the Neoproterozoic growth of western Gondwana occurred firstly during the Late Tonian and Cryogenian (950–750 Ma), through the development of intraoceanic juvenile arcs, suggesting the presence of a large ocean separating the São Francisco and Amazonian/West African and Saharan cratons. In Hoggar, within the Silet region (Algeria), diorite–tonalite and monzogranite plutons from the Iskel magmatic arc yielded U-Pb zircon ages at ca. 868 and 839 Ma (Caby et al., 1982). Occurrence of slices of pre-Pan-African basement directly overlain by shelf sediments and capped by arc volcanic rocks in several localities suggests that the Iskel magmatic arc was built on attenuated continental crust adjacent to possible slices of oceanic lithosphere (Caby, 2003; Lapierre et al., 1986). Further south, in the Gourma region (Mali) the Tilemsi-Amalaoulaou intraoceanic arc assemblages (Dostal et al., 1994) were dated within the 790–710 Ma time interval (Berger et al., 2011; Caby, 1989). The Tilemsi arc is considered the upper crust supra-structure equivalent of the Amalaoulaou complex (Berger et al., 2011). Although precise geochronological data is lacking for the Kabyé massif in the Dahomeyan belt (Togo), geochemical and field characteristics suggest that this massif could in fact represent the roots of a continental arc (Duclaux et al., 2006).

In Africa the active continental margin (Andean-type) is located in the east of the oceanic terranes (Berger et al., 2011; Caby, 2003). This stage of ocean-continent subduction was dated at 696 ± 5 Ma within the Kindal Terrane and at 716 ± 6 Ma in the Idras des Iforas region in Mali (Bruguier et al., 2008; Caby and Andreopoulos-Renaud, 1987), indicating that it was partially coeval with the ocean–ocean subduction stage active further west. In Central Brazil, the Neoproterozoic Goiás magmatic arc in the Brasilia Belt is composed of juvenile orthogneisses ranging from ca. 920 to 780 Ma (Laux et al., 2005; Matteini et al., 2010; Pimentel and Fuck, 1992). Younger ages at ca. 670–630 Ma were

Fig. 8. A. K_2O versus SiO_2 diagram of Peccerillo and Taylor (1976), showing that granitoids are high-K calc-alkaline to shoshonitic in nature. B. A/NK vs. ASI diagram modified from Shand (1947). C. Rb versus Ta + Yb tectonic discrimination diagram of Pearce et al. (1984). D. Th/Hf versus Ta/Hf discrimination diagram between continental active margins and within plate volcanic zones of Schandl and Gorton (2002).

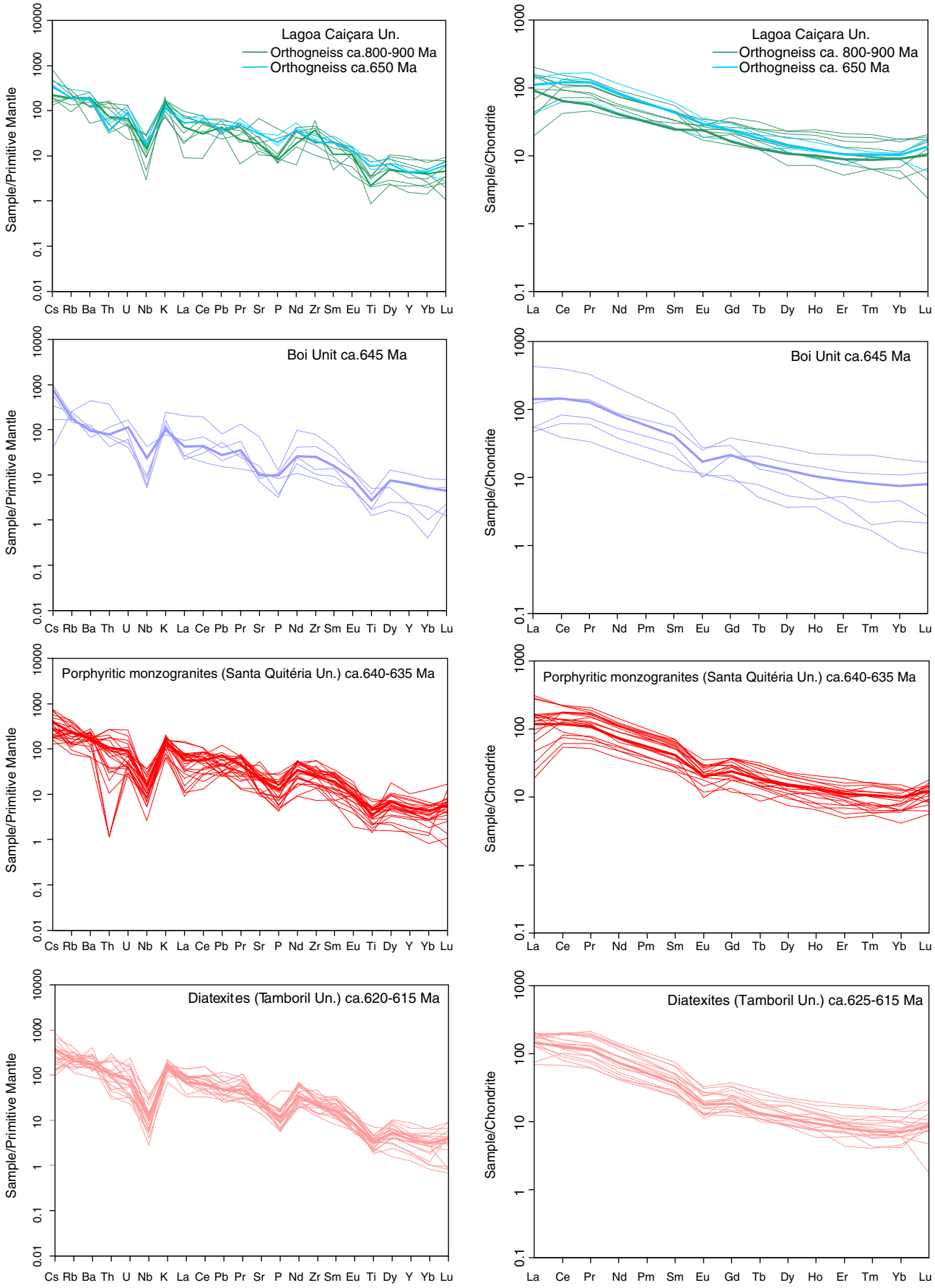

Fig. 9. Spider diagrams of trace elements and REE for granitoid rocks of the protolith of granitoids and migmatites from Tamboril-Santa Quitéria Complex. Primitive mantle and Chondrite normalized values from McDonough and Sun (1995) and Sun and McDonough (1989), respectively.

also reported (Laux et al., 2005) and may represent a second stage of the pre-collisional magmatism in Central Brazil, also with hybrid mantle–crustal isotopic signatures.

In other words, the juvenile nature of these rocks in the CCD and geological relationships along the orogen in Africa and Central Brazil suggest that the large Goiás-Pharusian Ocean was connected and did not narrow into a small ocean in the Borborema Province as suggested by some authors (Brito Neves and Fuck, 2013; Castaing et al., 1994; Neves, 2003).

4.1.2. Mature Andean-type arc magmatism: ca. 660–630 Ma

The granitoids of the younger magmatism marked by the Santa Quitéria and Boi units (samples DKE-211 and DKE-277) together with the gneissic granitoids found in the Lagoa Caiçara unit (samples DKE-269 and DKE-231) and granitoid schollen (samples DKE-170 and DKE-125A) found within the diatexites of the Tamboril unit, range in age between 663 and 627 Ma. These rocks have negative to positive $\varepsilon Hf_{(t)}$ (−18.7 to +13.2) and $\varepsilon Nd_{(t)}$ (−10.75 to +1.80) combined with moderate to high initial $^{87}Sr/^{86}Sr$ (0.7056–0.7143). Isotopic results for the granitoids within this 30 m.y. span of magmatism indicate sources ranging from mantle to continental (Table 2), which characterizes a mature arc stage.

After the juvenile granitoids of the 890–800 Ma arc, the oldest granitoid (663 ± 6.6 Ma, sample DKE-170) within the Tamboril-Santa Quitéria Complex occurs as a raft inserted in the Tamboril unit close to the contact with the Santa Quitéria unit. The $\varepsilon Hf_{(t)}$, $\varepsilon Nd_{(t)}$ and initial $^{87}Sr/^{86}Sr$ indicate that this granitoid was derived from the partial melting of depleted mantle sources (Figs. 10 and 11). However, high zircon $\delta^{18}O$ values (5.94–9.06‰) suggest that these juvenile magmas would have also interacted with (meta)sedimentary rocks that

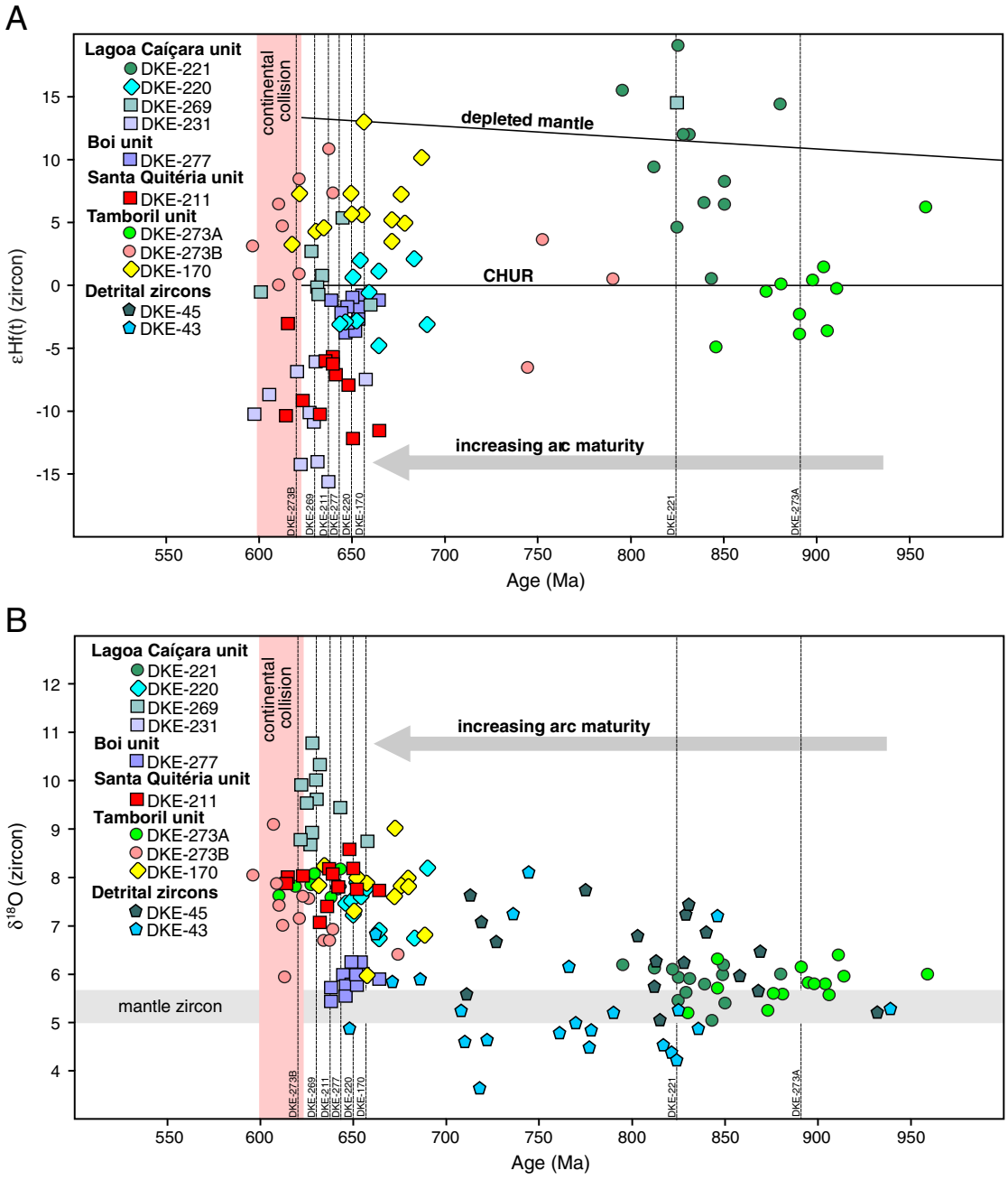

Fig. 10. A. Variations of $\delta^{18}O$ values with age for zircons from protolith of granitoids and migmatites from Tamboril-Santa Quitéria Complex. B. Schematic diagram for Lu-Hf isotopic evolution vs. U-Pb age for zircons from protolith of granitoids and migmatites from Tamboril-Santa Quitéria Complex.

contributed to increased $\delta^{18}O$ values. Sample DKE-170 contrasts with sample DKE-200A, the next oldest rock in this group, however. Sample DKE-200A is a mafic tonalite dated at 650.6 ± 5.1 Ma. Its isotopic composition indicates that old continental rocks were its main source (initial $^{87}Sr/^{86}Sr = 0.7105$; $\varepsilon Hf_{(t)} = -5.45$ and $\delta^{18}O$ 6.73–8.19, Table 2). The difference between the two samples is taken to indicate that contrasting sources (crust and mantle) were mobilized in this period. This is confirmed by the consideration of the remaining samples in this group.

The high-K to shoshonitic mafic dioritic and tonalitic rocks of the Boi unit are the oldest (648 ± 4.1 Ma, sample DKE-277) coherent and mappable magmatic rocks identified within the complex. While $\varepsilon Hf_{(t)}$ for sample DKE-277 is negative (−6.6 to −0.8) and suggestive of crust participation, juvenile $\varepsilon Nd_{(t)}$ signatures (Fetter et al., 2003), attest for mixing between rocks with mantle and crustal signatures. Mantle involvement is further supported by the zircon $\delta^{18}O$ values (5.48–6.25‰). The diorite gneiss of sample DKE-125A although lacking isotopic data, has a similar zircon U-Pb age of 646 ± 4.5 Ma and is correlated with the Boi unit magmatism.

The youngest magmatic intrusive pulses in the Tamboril-Santa Quitéria Complex are represented by the 632 ± 5.1 and 627 ± 4.9 Ma biotite granitic magmatism found in the Lagoa Caíçara unit. Nd-Sr isotopic data for these rocks are coherent with a crustal origin as also suggested by high zircon $\delta^{18}O$ values (6.73–10.82‰). Inherited zircons with ages at 823 ± 23, 796 ± 19 and 761 ± 19 Ma indicate that Early Neoproterozoic juvenile protoliths from the Lagoa Caíçara unit were also important sources for this granitic magmatism, and may have contributed to the partially positive $\varepsilon Hf_{(t)}$ in sample DKE-269.

As discussed above, one of the main features of the Santa Quitéria monzogranitic magmatism is the close association with syn-plutonic mafic dykes of enriched mantle affinity, likely connected with the Boi unit magmatism. This mantle input is geochemically enriched and predominantly shoshonitic in nature (Costa et al., 2013; Zincone, 2011). Available geochronological data for the high-K to shoshonitic porphyritic granites of the Santa Quitéria unit allow us to bracket its formation to within the 640–635 Ma time interval (Fetter et al., 2003 and our data). Negative $\varepsilon Hf_{(t)}$ (−12.2 to −2.9) and $\varepsilon Nd_{(t)}$ (−4.25) values together with high initial $^{87}Sr/^{86}Sr$ (0.7107) and high zircon $\delta^{18}O$ values (7.06–8.57‰) indicate that crust was involved in the formation of the Santa Quitéria monzogranites. The Boi and Santa Quitéria units are part of the same magmatic system and illustrate well the interaction of crust–mantle sources commonly described in mature arcs (DePaolo, 1981).

The enriched signatures observed in the Santa Quitéria-type granitoids could be explained by partial melting of a modified metasomatic mantle combined with significant crustal contamination, rather than an asthenosphere input. In many arcs magmas have enriched geochemical features, which are consistent with a derivation from mantle sources modified by metasomatic fluids. These fluids can be derived from subducted incompatible element-rich sediments (Tatsumi, 1986), or from slab melts (Martin et al., 2005). The relative roles of crustal contamination and mantle source enrichment (e.g. through the contribution of subducted terrigenous sediments or slab fluids) are often debated in arc petrogenesis (e.g. Fourcade et al., 1994), but difficult to quantify. The expected modifications in the underlying mantle would arise from the long-lasting interaction of subduction derived melts since the ca. 850 Ma, initiated by the Lagoa Caíçara juvenile magmatism.

Along the West Gondwana Orogen, other Andean-type arcs have also been identified in the time bracket between 650 and 600 Ma. As mentioned above, in Hoggar (Mali) such arc magmatism is related with the consumption of the Goiás-Pharusian Ocean by east–southeast directed subduction (Caby et al., 1981) and the formation of the large Adrar des Iforas continental arc batholith at around 630 Ma (Liégeois et al., 1987). In the Dahomey section of the orogen in Togo and Benin, arc-type Neoproterozoic granitoid rocks dated at ca. 650–630 Ma (Kalsbeek et al., 2012) are also related with an east-dipping subduction zone evolved during the consumption of the Goiás-Pharusian Ocean. Finally, in the central Brazil branch of the orogen, final magmatic pulses of the Goiás magmatic arc at ca. 630 Ma (Laux et al., 2005; Pimentel et al., 1999) could be correlated with this mature arc setting that predates final collision in the West Gondwana Orogen.

4.1.3. Reworking of arc rocks: the 620–610 Ma crustal anatexis event

Samples of neosome resulting from crustal anatexis define the youngest group of rocks within the complex at 625–610 Ma, generally grouped in the Tamboril unit. In the field the Tamboril magmatism results from the remelting of the surrounding protoliths (Fig. 5), mainly orthogneisses of intermediate compositions of the Lagoa Caíçara and Santa Quitéria units and minor metasedimentary rocks of the Ceará Complex.

The resulting magmatism in the Tamboril unit dated here at 625–618 Ma (samples DKE-273 and DKE-125) consists of neosomes and their isotopic composition reflects the variations of their source from juvenile to hybrids with some crustal input.

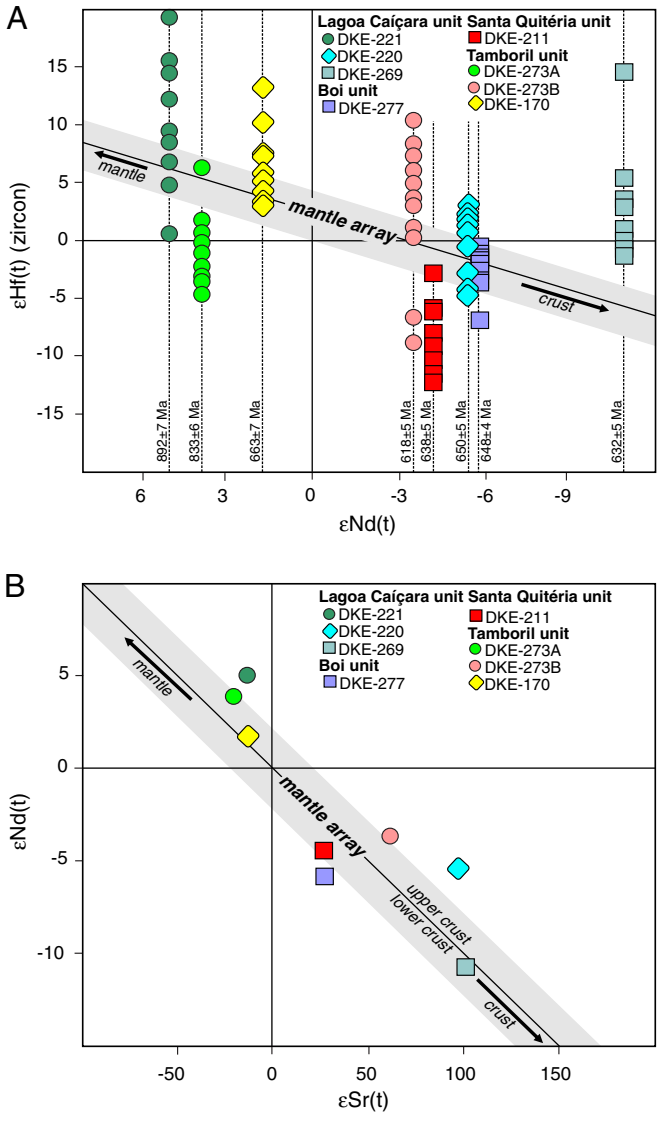

Fig. 11. A. Relationship between zircon $\varepsilon Hf(t)$ and whole-rock $\varepsilon Nd(t)$ for protolith of granitoids and migmatites from Tamboril-Santa Quitéria Complex. Mantle and crust arrays are from to Vervoort et al. (1999). B. $\varepsilon Nd(t)$ vs. $\varepsilon Sr(t)$ diagram protolith of granitoids and migmatites from Tamboril-Santa Quitéria Complex. The line separating materials derived from upper (high positive εSr) to lower crust (low positive εSr) was proposed by DePaolo and Wasserburg (1979).

The schollen diatexite sample DKE-273 suggests that it was derived from the partial melting of the juvenile rocks of the Lagoa Caíçara unit. Intermediate granitoids, such as those of the Lagoa Caíçara unit have no muscovite and small amounts of biotite or hornblende (10–25%), precluding generation of large melt fractions by dehydration melting (Sawyer, 2008). The large melt fraction and the lack of anhydrous phases in these migmatites, such as garnet, sillimanite, orthopyroxene or cordierite, suggest melting by influx of water close to the solidus temperature promoting water-saturated melting of quartz + plagioclase-K-feldspar (Kenah and Hollister, 1983; Sawyer, 1998, 2008). In support of this interpretation is the existence of peritectic hornblende in leucosomes in some sections of the Lagoa Caíçara unit (see sample DKE-221). Gardien et al. (2000) have demonstrated that the stability of hornblende formed from biotite breakdown requires the addition of external water.

Close investigation of our analyses of schollen and diatexitic granite of samples DKE-273A and 273B suggests however that other sources were also involved in the generation of melts surrounding the schollen. Although melting of the tonalitic/granodioritic paleosome and generation of the diatexite melt are evident in the field, zircon $\varepsilon Hf_{(t)}$ values diverge from the whole-rock $\varepsilon Nd_{(t)}$, suggesting Hf-Nd isotope decoupling in the diatexites (Fig. 11A). The behavior of the Lu-Hf system during melting is analogous to that of the Sm-Nd system, with the daughter elements Hf and Nd fractionating into the melt to a higher degree than the parent elements Lu and Sm (Scherer et al., 2007). Because Hf and Nd fractionate more strongly into melts than Lu and Sm, the melt will have lower Lu/Hf and Sm/Nd values than the protolith and over time the isotopic compositions of the melt and protolith will diverge into lower and higher $^{176}Hf/^{177}Hf$ and $^{143}Nd/^{144}Nd$ values, respectively. The $(^{176}Hf/^{177}Hf)_i$ values for the zircons of the diatexite of the Lagoa Caíçara unit are higher or equal to the $(^{176}Hf/^{177}Hf)_i$ of the source juvenile material (schollen), indicating that radiogenic ^{176}Hf remained constant or slightly increased during the melting event. We interpret this feature as a direct consequence of the isotopic inheritance of the juvenile source zircons to the melt-precipitated zircons. We believe that the Hf budget in the melt is being controlled mainly by the zircons with high $(^{176}Hf/^{177}Hf)_i$ derived from the juvenile protoliths and that rapid melting by the addition of water would preclude radiogenic ^{176}Hf to homogenize with other possible sources and thus reflect the direct isotopic composition of the protolith (Fig. 12). The decoupling of zircon Hf versus whole-rock Nd isotopes in the Lagoa Caíçara diatexites is due to the retention of radiogenic Hf during partial melting of juvenile arc-derived zircons, similarly suggested by Wu et al. (2006) for the reworking of juvenile crust in South China. Since the bulk ^{143}Nd is available from a variety of minerals and sources, rather than zircon which, is the main container of Hf in crustal rocks (Hoskin and Schaltegger, 2003) we believe that during partial melting the whole-rock Sm-Nd system was readily equilibrated with the new melt, and reflects the addition of other external, old continental sources that contributed to the lower and less radiogenic $\varepsilon Nd_{(t)}$ value. Hf provided by zircons from the external contaminants was minor compared with the Hf provided by the juvenile protolith, and this may reflect: i) low zircon fertility of crustal contaminants; ii) low magmatic resorbtion of these zircons in the melt; or iii) a bias introduced by our low resolution sampling. These external sources are also observed in the field as preserved schollen of metasedimentary rocks, granites and older Paleoproterozoic (2.1 Ga) orthogneisses from the basement.

The rapid addition of water during melting could explain the conservation of the protolith Hf isotopic signature of the melt-precipitated zircons as well as their high $\delta^{18}O$ values (Fig. 12). The origins of the fluids in geological processes are always intriguing and difficult to address. The time of diatexite formation is in agreement with the time of continental collision in Ceará Central Domain (see discussion below) and thus fluids associated with subducted material and underlying metasomatized mantle wedge are not possible sources. Instead, fluids released by prograde collisional metamorphic dehydration-type reactions of the adjacent rocks are suitable candidates, as proposed by White et al. (2005) at a smaller scale for the diatexites of Broken Hill, Australia.

4.1.4. Bracketing collision time

The fundamental question that arises when addressing temporal relationship of magmatic lineages of a given orogenic system, using the prefixes pre-, syn- and post-collisional is: *when did the collisional stage start*? Initial collision, starting at the first contact of the continental blocks, evolves into crustal thickening (due to plate overriding) followed much later by thinning due to gravitational adjustments in response to the delamination of crustal root (Leech, 2001). Each of these tectonic stages can be fingerprinted by a related tectono-thermal and magmatic manifestation preserved within the final orogenic record.

Retrogressed eclogitic rocks found between the western border of the Santa Quitéria Complex and the Transbrasiliano Lineament (Santos et al., 2009) are an essential piece of the collisional story of de orogen. Santos et al. (2013) reported the find of coesite inclusions within garnet, suggesting UHP (>2.7 GPa) metamorphic conditions at depths greater than 90 km. It is well known from recent collisional orogens, as well as in some fossil collisional zones, that eclogite facies metamorphism, including UHP rocks, is one the best markers of the onset of the collisional process (e.g. de Sigoyer et al., 2000; Gilotti, 2013; Leech et al., 2005; Liou et al., 2004; Liu et al., 2008). Petrochronology for the (U)HP metamorphism in the Forquilha eclogitic zone in CCD and along the West Gondwana Orogen in Togo and Mali indicates that the timing of continental collision was nearly synchronous for at least 2500 km along the orogen around 615–610 Ma (Ganade de Araujo et al., in revision).

Given the marked change in the nature of magmatism, from primary arc magma intrusion down to 625 Ma, to secondary magmatic rocks derived from the remelting of these primary magmatic rocks, at around 620–615 Ma, we postulate that this marks a change from early magmatism related to plate convergence associated with the consumption of the Goiás-Pharusian Ocean to crustal recycling due to collision.

The India-Asia collision is our type locality for large-scale continental collision. There collision started ca. 55 Ma (Klootwijk et al., 1992), ultimately creating the Himalaya and Tibet. The most obvious metamorphism occurred during partial melting ca. 20 Ma, but rare relict metamorphic minerals, textures, and isotope ages as old as 35–55 Ma attest to earlier Himalayan metamorphism (e.g., see Hodges, 2000; de Sigoyer et al., 2000). In the Himalayas ages for the coesite-bearing UHP eclogites are 45–55 Ma (de Sigoyer et al., 2000; Donaldson et al., 2013; Kaneko et al., 2003) while geochronology on the partially melted rocks indicates that melting was at 18–22 Ma (Harrison et al., 1998), constraining a gap of between 37 and 23 m.y. since the beginning of the collision and the main period of melting. Thus, widespread melting of mid-crustal levels is thought to have started at around 30 Ma, with more voluminous magmatism at around 20 Ma, and with melt present today ~15 km below the surface underneath the Tibetan Plateau (Harrison, 2006). Thermal modeling of crustal thickening suggests that the concomitant thickening of the layer enriched in heat producing elements leads to crustal heating generating crustal anatexis some tens of millions of years after crustal thickening in accordance to observations (England et al., 1988). This seems not to be the case in the Ceará Central Domain.

If our interpretation is correct, the change from arc magmatism to crustal anatexis occurred concurrently with collision suggesting one of several possibilities: a) the CCD is a deeper section of the collisional belt than the one presently exposed in the Himalayas, b) the thermal evolution of the exposed section of the CCD was different from that of the Himalayan front upon collision, with the CCD remaining hotter, or c) arrival of continental sediments into the subduction zone bringing water to the arc. Although melting was synchronous to the onset of

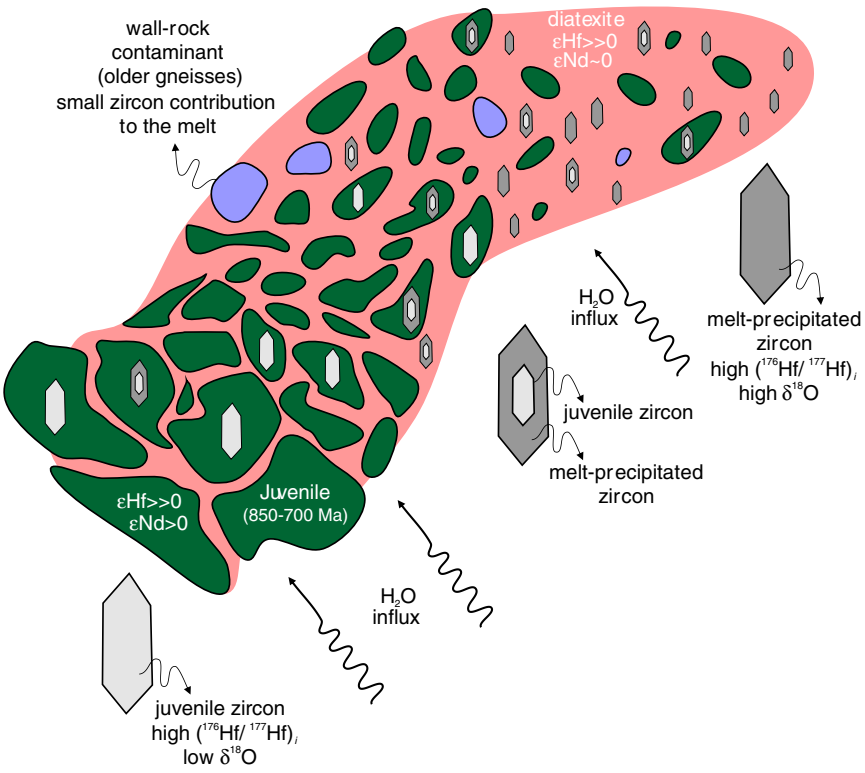

Fig. 12. Schematic illustration of the water-fluxed melting of juvenile protoliths. Hf budget in melt is mainly controlled by high initial ($^{176}Hf/^{177}Hf$) of juvenile arc-related protoliths, thus yielding a melt with high initial ($^{176}Hf/^{177}Hf$). Nd budget is controlled by mixing of juvenile protoliths and crustal contaminants yielding neutral εNd signatures in melt. Water-fluxed melting of juvenile protoliths is indicated by lack of anhydrous peritectic phases in melt, as well as by high $\delta^{18}O$ signatures.

collision in CCD, younger leucosomes containing anhydrous peritectic garnet and sillimanite derived from the partial melting of the metasedimentary rocks of the Ceará Complex were dated at 610–600 Ma (Arthaud, 2007; Castro, 2004) and possibly younger at 580 Ma (Fetter, 1999).

5. From a juvenile to mature arc setting and terminal collision

Our new data indicate that subduction initiation of the Goiás-Pharusian Ocean may have been active as early as 890 Ma in the Ceará Central Domain and, as suggested by detrital zircon studies from supracrustal rocks (Ganade de Araujo et al., 2012a), may have been continuous until terminal collision at ca. 620–615 Ma. However, the continuity of detrital zircon spectra contrasts with the apparent long pause between ca. 800 Ma and 660 Ma recorded by the magmatic rocks of the CCD alone. This apparent gap could be due to the erosion of the earlier arc granitoids or by insufficient geochronological data (Fig. 13).

In any case, the igneous samples investigated here record two main arc-building stages. The first, early to middle Neoproterozoic stage I, comprising mainly juvenile tonalites and granodiorites from the Lagoa Caíçara unit, followed by a second stage (stage II) that comprises abundant diorites, tonalites and mainly high-K monzogranites with mixed mantle–crustal signatures from the Santa Quitéria and Boi units and younger orthogneisses found in the Lagoa Caíçara unit.

The juvenile nature of the stage I arc granitoids suggests an initial emplacement outboard of the leading edge of the continental margin of the Paleoproterozoic-Archean basement of the Borborema Province to the east, at ca. 890 Ma possibly in an oceanic environment. This scenario is similar to that described in the earlier stages of Mesozoic convergent margin of Baja California, Mexico (Busby, 2004). In this area, the subducting Farallon plate at that time was old and cold at the trench and therefore the subduction zone was in retreat and the arc was thus emplaced in an extensional setting, generating intra-arc to backarc basins. Similarly, if the oceanic plate of the Pharusian-Goiás Ocean was old and cold at the time of subduction in the Ceará Central Domain an extensional setting would have developed between stage I arc and the former continental margin explaining for example the sediments deposited in the rear area of the arc in a possible back-arc setting between the juvenile Lagoa Caíçara unit and the Paleoproterozoic/Archean basement to east. However, provenance studies through detrital zircon investigation in these marine sediments of the Ceará Complex have both arc and continental signatures (Ganade de Araujo et al., 2012a) suggesting that stage I arc magmatism was not far off the continental margin (Fig. 14A and B). Furthermore, some authors have proposed that the bimodal alkaline (high-Nb) and mafic magmatism associated with these sediments between 840 and 750 Ma is related to extension (Arthaud, 2007; Arthaud et al., 2008; Castro, 2004). Imprecise upper intercept ID-TIMS U-Pb zircon ages at ca. 840 Ma from alkaline rhyolites with high-Nb content close to Itataia town (Castro, 2004) and ID-TIMS U-Pb zircon ages of 772 Ma from felsic gneissic sheets found further south close to Independência town may constrain the period of extension.

Development of a back-arc basin during stage I arc magmatism and extension of the continental crust to the east of the Lagoa Caíçara unit, generated space that was filled with progradational back-arc deposits that record arc growth above sea level to the west (Fig. 14B). No clear evidence is available to say if the back-arc basin developed into an incipient oceanic crust, however the mafic rocks close to Pentecoste town could be candidates and should be studied in detail.

The mature arc stage II magmatism is comprised of several pulses of granitoids and overprints magmatism related to stage I between 660–630 Ma (Castro, 2004; Fetter et al., 2003; Ganade de Araujo et al., 2012b) (Fig. 14C). These magmatic rocks are geochemically enriched when compared with the intermediate granitoids of stage I (Fig. 8A). Likewise, contrasting to the stage I granitoids, isotopic signatures of

stage II rocks show variable mixtures between juvenile and crustal material.

We postulate that after the last pulse of arc magmatism at ca. 627 Ma (sample DKE231), initial continent–continent collision in Ceará Central Domain is marked by the first contact between the stretched passive margin of Paleoproterozoic-Archean basement to the east (the Northern Borborema basement) and the Paleoproterozoic basement to the west (the Parnaíba + Granja Complex). Continental subduction is evidenced by the (U)HP eclogitic metamorphism in the Forquilha HP domain, which may have initiated as early as ca. 624 Ma reaching peak P conditions at ca. 615 Ma (Ganade de Araujo et al., in revision) (Fig. 14D). At this stage remelting of the arc assemblages took place in the Tamboril-Santa Quitéria Complex.

Eclogites and HP gneisses were also described in the back-arc basin in the vicinity of the Itataia town (Arthaud, 2007; Castro, 2004) and could be related to the west-dipping incipient subduction of the back-arc basin and stretched Paleoproterozoic continental crust during collision.

Images of the deep electrical structure across the Tamboril-Santa Quitéria Complex revealed two resistive features dipping from the upper crust into the upper mantle in downward convergence interpreted as the remnants of former subduction slabs (Padilha et al., 2014). However, in their northernmost magnetotelluric profile (closer to the study area) the images of these two resistive structures are not clear and the profile is characterized by a conductive east-dipping slab to the west of the Tamboril-Santa Quitéria Complex (Fig. 2 in Padilha et al., 2014).

The east-dipping resistive/conductive slab images between the Transbrasiliano Lineament and the arc rocks of the Tamboril-Santa Quitéria Complex are in agreement with the position of the (U)HP eclogites of Forquilha zone. We expect that the eastward subducting cold and dense slab of the oceanic crust was responsible for the mature arc stage magmatism at 660–630 Ma and pulled the attached continental crust to mantle pressures at ca. 615 Ma as recorded by the age of (U)HP metamorphism (Ganade de Araujo et al., in revision). This eastward subduction polarity has been also proposed to explain the geometry of supracrustal structure in other sectors of the West Gondwana Orogen (e.g. Caby, 2003; Duclaux et al., 2006; Liégeois et al., 1987), thus indicating an extensive eastward dipping subduction system during the Neoproterozoic.

The period following continental subduction at ca. 615 Ma is related to exhumation of the (U)HP eclogites, especially those found at the Forquilha (U)HP domain. The emplacement of the (U)HP rocks into shallower crustal levels was probably facilitated by extensional tectonics and buoyancy-aided exhumation (Fig. 14E).

6. Conclusions

The Ceará Central Domain of the Borborema Province is a Neoproterozoic orogenic area (Brito Neves et al., 2000), part of the 5000 km-long West Gondwana Orogen (Ganade de Araujo et al., 2014), which extends from Algeria in Africa to Central Brazil. Our results allowed the determination of three stages of magmatism reflecting three distinct tectonic environments: i) an early period of essentially juvenile arc magmatism at ca. 880–800 Ma, ii) a second, mature arc period between 660 and 630 Ma, characterized by hybrid mantle–crustal components, and iii) remelting of the arc-related igneous rocks during continental collision, evidenced by abundant extensive migmatization dated to between 625 and 600 Ma. These ages overlap with those of (U)HP eclogitic metamorphism at 624–615 Ma suggesting that migmatization occurred during continental subduction in a continent–continent collisional setting. The apparent gap between the two periods of arc magmatism could be explained by incomplete exposure and erosion. Evidence for continuous magmatism comes from abundant detrital zircons in the fore- and back-arc basins with ages in the range of 900 to 650 Ma. Oxygen isotopes from detrital zircons in the fore-arc

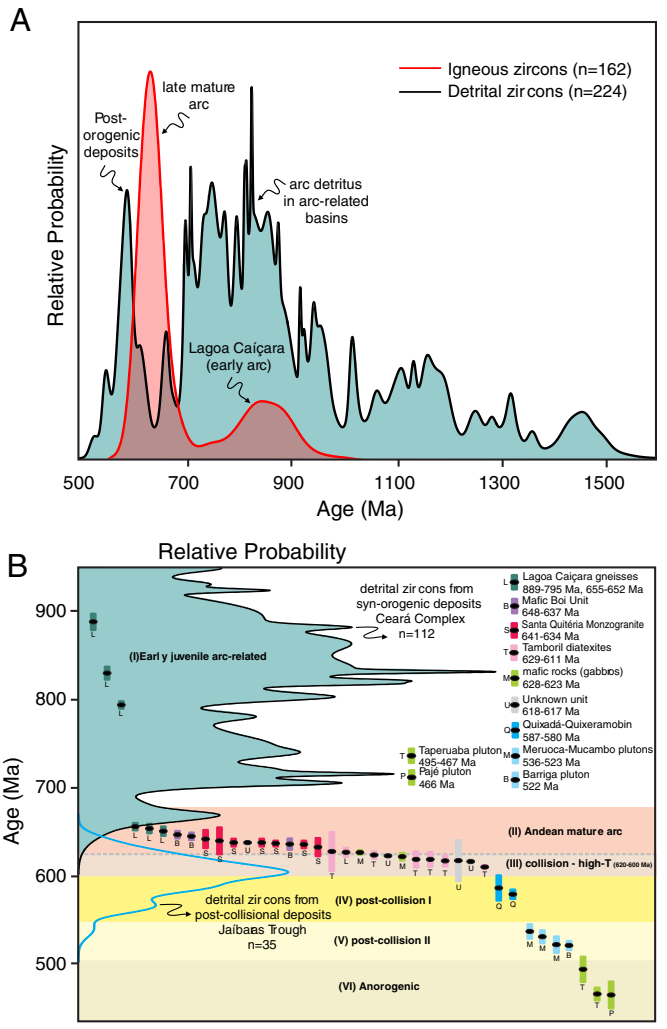

Fig. 13. A. Comparison between zircon ages acquired from the granitoids of Tamboril-Santa Quitéria in this study versus detrital zircons from back arc and fore arc basins from Ceará Complex (data from the detrital zircons from Ganade de Araujo et al., 2012a). B. Summary of magmatic ages of granitoid rocks of the Tamboril-Santa Quitéria Complex.

indicate that juvenile input persisted throughout the entire evolution of convergent magmatism. Igneous rocks of the Tamboril-Santa Quitéria Complex record a long-lived history of convergent magmatism lasting up to 350 m.y.

Supplementary data to this article can be found online at http://dx.doi.org/10.1016/j.lithos.2014.05.015.

Acknowledgments

CEGA is grateful to Izabel Ruiz for the help and guidance with the Sr-Nd analysis and to João Naleto for the field support and to Felipe Costa for fruitful geological discussions. CEGA, UGC and MASB are thankful to the financial support of São Paulo Research Foundation (FAPESP) 2012/00071-2 and to the Brazilian National Research Council (CNPq) for the grant 246206/2012-8 to CEGA. This is a contribution to the IGCP-628, Gondwana Map Project. This manuscript has benefited from the comments and suggestions of Cin-Ty Lee, Nelson Eby and an anonymous reviewer.

Appendix A. Analytical procedures

In order to better understand the temporal evolution and the source of different magmas we carried out in situ U-Pb zircon geochronology

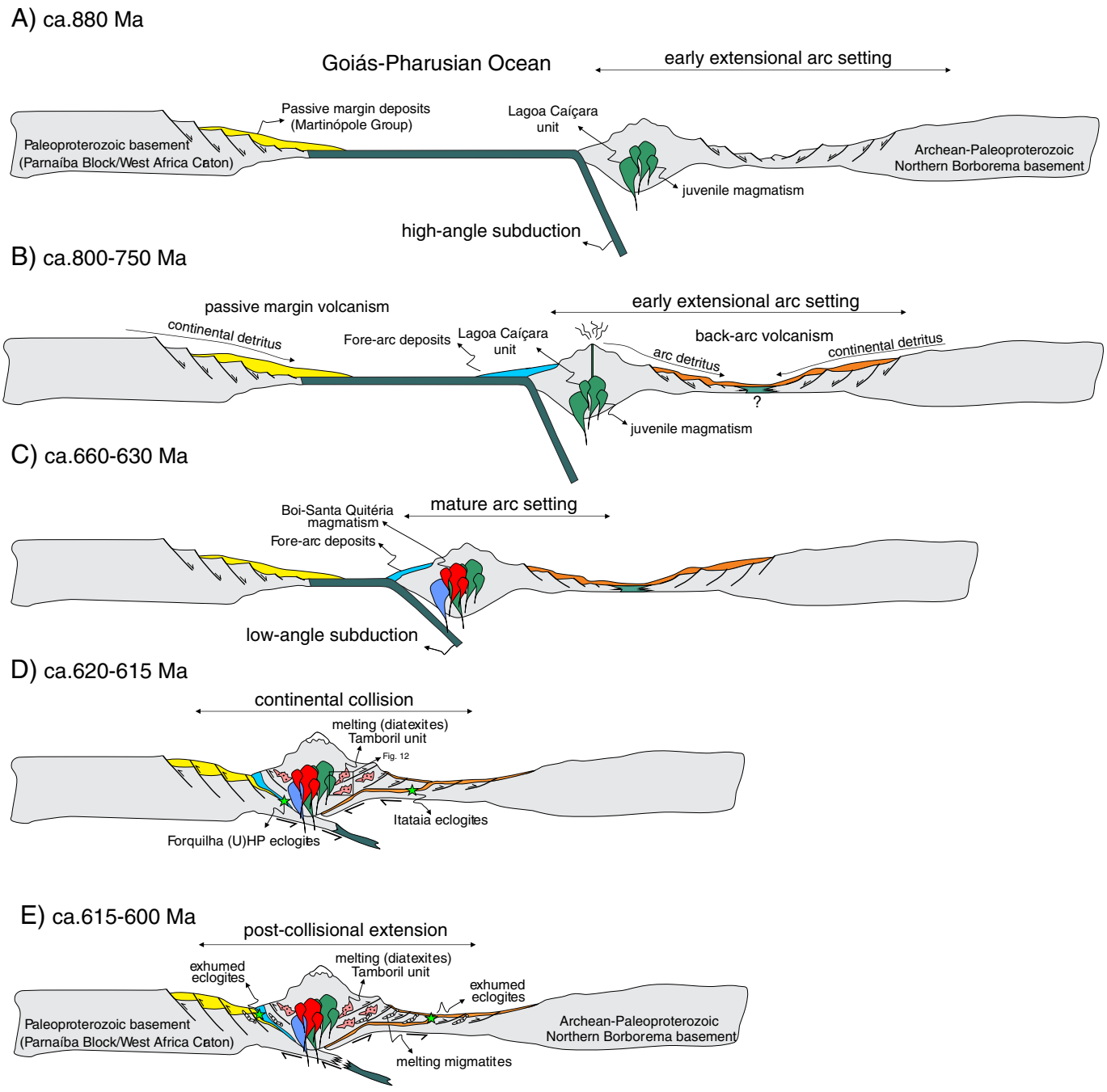

Fig. 14. Tectonic model for Neoproterozoic evolution for the continental convergent margin of Ceará Central Domain. A. Early subduction stage in an extensional setting, due to old oceanic lithosphere subduction and juvenile magmatism accretion on a stretched continental margin. B. Continuous subduction with development of extensional back-arc basins with associated magmatism and both arc- and continental-derived detritus. C. Compressive arc-setting and development of the Santa Quitéria arc. D. Terminal collision with subduction of stretched continental crust to the west of the Santa Quitéria arc and subduction of the stretched continental crust (e.g. back-arc basin) to the east of the Santa Quitéria arc. Collisional metamorphism on both sides of the arc is evidenced by (U)HP-eclogite rocks of Forquilha (Santos et al., 2009, 2013; Ganade de Araujo et al., in revision) and Itataia HP eclogites (Castro, 2004). E. Post-collision extension and exhumation of the (U)HP and HP rocks.

coupled with Hf and O isotopes on the same dated zircon domains. Zircon isotopic data were complemented by whole-rock Nd and Sr isotopes to better constrain granite sources for the same representative samples used for zircon investigation.

Zircons were separated from fresh crushed rocks (3–5 kg) using conventional and heavy liquid and magnetic techniques (jaw crusher, disk grinder, Wilfley table, Frantz isodynamic magnetic separator and density separation using bromoform and methylene iodite). Around 50–80 zircons from each sample were mounted in epoxy resin, polished to half of mean grain thickness for further imaging with transmitted light and cathodo-luminescence to unravel internal complexities. Cathodo-luminescence (CL) images of zircons were obtained using a Quanta 250 FEG electron microscope equipped with Mono CL3 + cathodo-luminescence spectroscope (Centaurus) at the Geochronological Research Center in São Paulo University, Brazil.

U-Pb analyses were done using SHRIMP IIe at the Geochronological Research Centre (CPGeo) at the São Paulo University. The data have been reduced in a manner similar to that described by Williams (1998 and references therein), using the SQUID Excel Macro of Ludwig (2001). Uncertainties given for individual U-Pb analyses (ratios and

ages) are at the 1σ level, however uncertainties in the calculated weighted mean ages are reported as 95% confidence limits and include the uncertainties in the standard calibrations where appropriate. For the age calculations, corrections for common Pb were made using the measured ^{204}Pb and the relevant common Pb compositions from the Stacey and Kramers (1975) model. Concordia plots, regressions and any weighted mean age calculations were carried out using Isoplot/Ex 3.0 (Ludwig, 2003) and where relevant include the error in the standard calibration. U-Pb geochronological results are presented in Table S1 of Supplementary data.

Lu-Hf analyses were also carried out at the Geochronological Research Centre (CPGeo) at the São Paulo University on a Neptune laser-ablation multi-collector inductively coupled plasma mass spectrometer equipped with a Photon laser system. The laser spot used was 39 μm in diameter with an ablation time of 60 s, repetition rate of 7 Hz, and He used as the carrier gas (Sato et al., 2009). $^{176}Hf/^{177}Hf$ ratios were normalized to $^{179}Hf/^{177}Hf = 0.7325$. Zircon Hf isotopic data are presented in Table 3. The isotopes ^{172}Yb, ^{173}Yb, ^{175}Lu, ^{177}Hf, ^{178}Hf, ^{179}Hf, ^{180}Hf, and $^{176}(Hf + Yb + Lu)$ were simultaneously measured. $^{176}Lu/^{175}Lu$ ratio of 0.02669 was used to calculate $^{176}Lu/^{177}Hf$. Mass bias corrections of Lu-Hf isotopic ratios were done applying the variations of GJ1 standard. A decay constant for ^{176}Lu of 1.867×10^{-11} (Söderlund et al., 2004), the present-day chondritic ratios of $^{176}Hf/^{177}Hf = 0.282772$ and $^{176}Lu/^{177}Hf = 0.0332$ (Blichert-Toft and Albarede, 1997) were adopted to calculate εHf values. A two-stage continental model (T_{DM}) was calculated using the initial $^{176}Hf/^{177}Hf$ of zircon and the $^{176}Lu/^{177}Hf = 0.022$ ratio for the lower continental crust (Griffin et al., 2004). Zircon Lu-Hf isotopic results are presented in Table S2 of Supplementary data.

Oxygen isotopic compositions were obtained in three separate analytical sessions using the SHRIMP-II equipped with a Cs-gun at the Research School of Earth Science (RSES) in The Australian National University as described by Ickert et al. (2008). TEMORA 2 zircon ($\delta^{18}O = 8.2‰$; Black et al., 2004) was analyzed along with FC1 zircon. The results are presented in Table S3 of Supplementary data and plotted on Fig. 10A. No corrections for IMF/gain drift or EISIE were necessary. Oxygen isotope analyses of FC1 on SHRIMP II, normalized to TEMORA 2, yield a mean $\delta^{18}O$ value of 5.5 ± 0.3‰.

Nd-Sr isotopic compositions were determined by thermal ionization mass spectrometry (TIMS) in a VG354 spectrometer equipped with a single Faraday detector at the Geochronological Research Centre (CPGeo) at the São Paulo University. The same powders used for whole-rock elemental analyses were taken into solution by acid digestion, and the elements of interest were separated in ion-exchange columns following the procedures described by Sato et al. (1995). No spikes were added; $^{87}Rb/^{86}Sr$ and $^{147}Sm/^{144}Nd$ ratios were calculated from whole-rock analyses obtained by XRF (Rb and Sr) and ICP-MS (Sm and Nd). Nd-Sr isotopic results are presented in Table S4 of Supplementary data.

Major and trace elements, were analyzed at the SGS GEOSOL laboratories according to the package used by the Geological Survey of Brazil. Major element oxides were determined using a Varian Vista Pro ICP-AES. Trace elements were determined using a Perkin-Elmer Sciex ELAN 6000 ICP-MS. Analyses of USGS rock standards (BCR-2, BHVO-1 and AGV-1) indicate precision and accuracy better than 1% for major elements and 5% for trace elements and REE. Whole rock geochemical results are presented in Table S5 of Supplementary data.

References

Amaral, W.S., 2010. Análise Geoquímica, Geocronológica e Geotermobarométrica das Rochas de alto grau Metamórfico Adjacentes ao arco Magmático de Santa Quitéria, NW da Província Borborema. (PhD thesis) Universidade Estadual de Campinas, Campinas (210 pp.).

Ancelmi, M.F., dos Santos, T.J.S., Reginato, R.A., Amaral, W.S., Monteiro, L.V.S., 2013. Geologia da faixa Eclogítica de Forquilha, Domínio Ceará Central, noroeste da Província Borborema. Brazilian Journal of Geology 43, 235–252.

Arthaud, M.H., 2007. Evolucão Neoproterozóica do Grupo Ceará (Domínio Ceará Central, NE Brasil): Da Sedimentacão à Colisão Continental Brasiliana. (PhD thesis) Universidade de Brasília, Brasília (170 pp.).

Arthaud, M.H., Caby, R., Fuck, R.A., Dantas, E.L., Parente, C.V., 2008. Geology of the Northern Borborema Province, NE Brazil and its correlation with Nigeria, NW Africa. In: Pankhurst, R.J., Trouw, R.A.J., Brito Neves, B.B., De Wit, M.J. (Eds.), West Gondwana: Pre Cenozoic Correlations Across the Atlantic Region. Geological Society, London, Special Publications 294, 49–67.

Bard, J.P., 1983. Metamorphism of an obducted island arc: example of the Kohistan sequence (Pakistan) in the Himalayan collided range. Earth and Planetary Science Letters 65, 133–144.

Berger, J., Caby, R., Liégeois, J.P., Mercier, J.C.C., Demaiffe, D., 2011. Deep inside a Neoproterozoic intra-oceanic arc: growth, differentiation and exhumation of the Amalaoulaou complex (Gourma, Mali). Contributions to Mineralogy and Petrology 162, 773–796.

Black, L.P., Kamo, S.L., Allen, C.M., Davis, D.W., Aleinikoff, J.N., Valley, J.W., Mundil, R., Campbell, I.H., Korsch, R.J., Williams, I.S., Foudoulis, C., 2004. Improved Pb-206/U-218 microprobe geochronology by the monitoring of a trace-element-related matrix effect; SHRIMP, ID-TIMS, ELA-ICP-MS and oxygen isotope documentation for a series of zircon standards. Chemical Geology 205, 115–140.

Blichert-Toft, J., Albarede, F., 1997. The Lu-Hf isotope geochemistry of chondrites and the evolution of the mantle–crust system. Earth and Planetary Sciences Letters 148, 243–258.

Brito Neves, B.B., Cordani, U.G., 1991. Tectonic evolution of South America during the Late Proterozoic. In: Stern, R.J., Van Schmus, W.R. (Eds.), Crustal Evolution in the Late Proterozoic. Precambrian Research 53, 23–40.

Brito Neves, B.B., Fuck, R., 2013. Neoproterozoic evolution of the basement of the South-American platform. Journal of South American Earth Sciences 47, 72–89.

Brito Neves, B.B.de., Santos, E.J., Van Schmus, W.R., 2000. Tectonic History of the Borborema Province, NW Brazil. In: Cordani, U.G., Milani, E.J., Thomaz Filho, A., Campos, D.A. (Eds.), Tectonic Evolution of South America, pp. 151–182 (Rio de Janeiro).

Bruguier, O., Bosch, D., Caby, R., Galland, B., Hammor, D., 2008. Sampling an active continental paleomargin: a LA-ICP-MS U-Pb zircon study from the Adrar des Iforas (Mali). Geochimica et Cosmochimica Acta 72, A118.

Burg, J.P., Bodinier, J.L., Chaudhry, S., Hussain, S., Dawood, H., 1998. Infra-arc mantle–crust transition and intra-arc mantle diapirs in the Kohistan Complex (Pakistani Himalaya): petro-structural evidence. Terra Nova 10, 74–80.

Busby, C., 2004. Continental growth at convergent margins facing large ocean basins: a case study from Mesozoic convergent-margin basins of Baja California, Mexico. Tectonophysics 392, 241–277.

Caby, R., 1989. Precambrian terranes of Benin Nigeria and Northeast Brazil and Late Proterozoic South Atlantic fit. Geological Society of America, Special Paper 230, 145–158.

Caby, R., 2003. Terrane assembly and geodynamic evolution of central-western Hoggar: a synthesis. Journal of African Earth Sciences 37, 133–159.

Caby, R., Andreopoulos-Renaud, U., 1987. Le Hoggar oriental, bloc cratonisé à 730 Ma dans la chaîne pan-africaine du nord du continent Africain. Precambrian Research 36, 335–344.

Caby, R., Arthaud, M.H., 1986. Major Precambrian nappes of the Brazilian belt, Ceará, northeast Brazil. Geology 14, 871–874.

Caby, R., Betrand, J.M.L., Black, R., 1981. Oceanic Closure and Continental Collision in the Hoggar-Iforas-Pan-African segment. In: Kroner, A. (Ed.), Precambrian Plate Tectonics. Elsevier, Amsterdam, pp. 407–434.

Caby, R., Andreopoulos-Renaud, U., Gravelle, M., 1982. Cadre Geologique et Geochronologie U/Pb sur Zircon des Batholites Precoces Dans le Segment Pan-Africain du Hoggar Central (Algerie). Bulletin de la Societe Geologique de France 24, 677–684.

Castaing, C., Feybesse, J.A., Thiéblemont, D., Triboulet, C., Chevremont, P., 1994. Palaeogeographical reconstructions of the Pan-African/Brasiliano orogen: closure of an oceanic domain or intracontinental convergence between major blocks? Precambrian Research 69, 327–344.

Castro, N.A., 2004. Evolução Geológica Proterozóica da região entre Madalena e Taperuaba, Domínio Tectônico Ceará Central (Província Borborema). Instituto de Geociências, Universidade de São Paulo PhD thesis, 221 p.

Castro, N.A., Ganade de Araujo, C.E., Basei, M.A.S., Osako, L.S., Nutman, A., Liu, D., 2012. Ordovician A-type granitoid magmatism on the Ceará Central Domain, Borborema Province, NE-Brazil. Journal of South American Earth Sciences 36, 18–31.

Cavalcante, J.C., Vasconcelos, A.M., Medeiros, M.F., Paiva, I.P., Gomes, F.E.M., Cavalcante, S. N., Cavalcante, J.E., Melo, A.C.R., Duarte Neto, V.C., Bevenides, H.C., 2003. Mapa Geológico do Estado do Ceará – Escala 1:500.000. CPRM-SGB Servico Geológico do Brasil, Fortaleza.

Cordani, U.G., Pimentel, M.M., Ganade de Araújo, C.E.G., Basei, M.A.S., Fuck, R.A., Girardi, V. A.V., 2013a. Was there an Ediacaran Clymene Ocean in central South America? American Journal of Science 313, 517–539.

Cordani, U.G., Pimentel, M.M., Ganade de Araújo, C.E.G., Fuck, R.A., 2013b. The significance of the Transbrasiliano-Kandi tectonic corridor for the amalgamation of West Gondwana. Brazilian Journal of Geology 43, 583–597.

Costa, F.G., Ganade de Araújo, C.E., Amaral, W.D.S., Vasconcelos, A.M., Rodrigues, J.B., 2013. Idade U-Pb (LA-ICPMS) em zircão e isótopos de Nd para granitoides do Complexo Tamboril-Santa Quitéria, Domínio Ceará Central: implicações para magmatismo neoproterozoico sin-colisional no domínio norte da Província Borborema. Geologia USP Série Científica 13, 159–174.

de Sigoyer, J., Chavagnac, V., Blichert-Toft, J., Villa, I.M., Luais, B., Guillot, S., Mascle, G., 2000. Dating the Indian continental subduction and collisional thickening in the northwest Himalaya: multichronology of the Tso Morari eclogites. Geology 28, 487–490.

De Wit, M.J., Brito Neves, B.B., Trouw, R.A.J., Pankhurst, R.J., 2008. Pre-Cenozoic correlations across the South Atlantic region: the ties that bind. In: Pankhurst, R.J., Trouw, R.A.J., Brito Neves, B.B., De Wit, M.J. (Eds.), West Gondwana: Pre-Cenozoic Correlations Across the Atlantic Region. Geological Society, London, Special Publications 294, 1–8.
DePaolo, D.J., 1981. A neodymium and strontium isotopic study of the Mesozoic calc-alkaline granitic batholiths of the Sierra Nevada and Peninsular Ranges, California. Journal of Geophysical Research: Solid Earth 86, 10470–10488.
DePaolo, D.J., Wasserburg, G.J., 1979. Sm-Nd age of the Stillwater Complex and the mantle evolution curve for neodymium. Geochimica et Cosmochimica Acta 43, 999–1008.
DePaolo, D.J., Linn, A.M., Schubert, G., 1991. The continental crustal age distribution: method of determining mantle separation ages from Sm-Nd isotopic data and application to the southwestern United States. Journal of Geophysical Research 96, 2071–2088.
Donaldson, D.G., Webb, A.A.G., Menold, C.A., Kylander-Clark, A.R., Hacker, B.R., 2013. Petrochronology of Himalayan ultrahigh-pressure eclogite. Geology 41, 835–838.
Dostal, J., Dupuy, C., Caby, R., 1994. Geochemistry of the Neoproterozoic Tilemsi belt of Iforas (Mali, Sahara): a crustal section of an oceanic island arc. Precambrian Research 65, 55–69.
Duclaux, G., Ménot, R.P., Guillot, S., Agbossoumondé, Y., Hilairet, N., 2006. The mafic layered complex of the Kabye massif (north Togo and north Benin): evidence of a Pan-African granulitic continental arc root. Precambrian Research 151, 101–118.
England, P.C., Houseman, G.A., Osmaston, M.F., Ghosh, S., 1988. The mechanics of the Tibetan Plateau [and discussion]. Philosophical Transactions of the Royal Society of London, Mathematical and Physical Sciences 326, 301–320.
Fetter, A.H., 1999. U/Pb and Sm/Nd Geochronological Constraints on the Crustal Framework and Geologic History of Ceará State, NW Borborema Province, NE Brazil: Implications for the Assembly of Gondwana. (PhD thesis) Kansas University.
Fetter, A.H., Van Schmus, W.R., Santos, T.J.S., Arthaud, M.H., Nogueira Neto, J.A., 2000. U-Pb and Sm-Nd geochronological constraints on the crustal evolution and basement architecture of Ceará State, NW Borborema Province, NE Brazil: implications for the existence of the Paleoproterozoic supercontinent Atlantica. Revista Brasileira de Geociencias 30, 102–106.
Fetter, A.H., Santos, T.J.S., Van Schumus, W.R., Hackspacher, P.C., Brito Neves, B.B., Arthaud, M.H., Nogueira Neto, J.A., Wernick, E., 2003. Evidence for Neoproterozoic continental arc magmatism in the Santa Quitéria Batholith of Ceará State, NW Borborema Province, NE Brazil: implications for the assembly of west Gondwana. Gondwana Research 6, 265–273.
Fourcade, S., Maury, R., Defant, M.J., McDermott, F., 1994. Mantle metasomatic enrichment versus arc crust contamination in the Philippines: oxygen isotope study of Batan ultramafic nodules and northern Luzon arc lavas. Chemical Geology 114, 199–215.
Ganade de Araujo, C.E.G., Costa, F.G., Pinéo, T.R.G., Cavalcante, J.C., Moura, C.A.V., 2012. Geochemistry and 207Pb/206Pb zircon ages of granitoids from the southern portionof the Tamboril-Santa Quitéria granitic-migmatitic complex, Ceará Central Domain, Borborema Province (NE Brazil). Journal of South American Earth Sciences 33, 21–33.
Ganade de Araujo, C.E.G., Cordani, U.G., Basei, M.A., Castro, N.A., Sato, K., Sproesser, W.M., 2012a. U-Pb detrital zircon provenance of metasedimentary rocks from the Ceará Central and Médio Coreaú Domains, Borborema Province, NE-Brazil: tectonic implications for a long-lived Neoproterozoic active continental margin. Precambrian Research 206, 36–51.
Ganade de Araujo, C.E., Cordani, U.G., Basei, M.A.S., Sato, K., 2012b. Arc reworking During Collision: Combined Lu-Hf LA-ICP-MS and U-Pb SHRIMP Results From the Tamboril-Santa Quit_eria Complex, NE Brazil. In: Kositcin, N., Bodorkos, S. (Eds.), 6th International SHRIMP Workshop - Program and Abstracts. Geoscience Australia, Canberra (Record 2012/52).
Ganade de Araujo, C.E., Rubatto, R., Hermann, J., Cordani, U.G., Caby, R., Basei, M.A.S. (in revision). Evidence for >2500-km-long contemporaneous deep continental subduction in the West Gondwana Orogen, Nature Communications.
Ganade de Araujo, C.E., Weinberg, R.F., Cordani, U.G., 2014. Extruding the Borborema Province (NE-Brazil): a two-stage Neoproterozoic collision process. Terra Nova 26, 157–168.
Gardien, V., Thompson, A.B., Ulmer, P., 2000. Melting of biotite + plagioclase + quartz gneisses: the role of H_2O in the stability of amphibole. Journal of Petrology 41, 651–666.
Gilotti, J.A., 2013. The realm of ultrahigh-pressure metamorphism. Elements 9, 255–260.
Griffin, W.L., Belousova, E.A., Shee, S.R., Pearson, N.J., O'Reilly, S.Y., 2004. Archean crustal evolution in the northern Yilgarn Craton: U-Pb and Hf isotope evidence from detrital zircons. Precambrian Research 131, 231–282.
Harrison, T.M., 2006. Did the Himalayan Crystallines extrude partially molten from beneath the Tibetan Plateau? Geological Society, London, Special Publications 268, 237–254.
Harrison, T.M., Grove, M., Lovera, O.M., Catlos, E.J., 1998. A model for the origin of Himalayan anatexis and inverted metamorphism. Journal of Geophysical Research: Solid Earth 103, 27017–27032.
Hawkesworth, C.J., Kemp, A.I.S., 2006. Using hafnium and oxygen isotopes in zircons to unravel the record of crustal evolution. Chemical Geology 226, 144–162.
Hildreth, W., Moorbath, S., 1988. Crustal contributions to arc magmatism in the Andes of central Chile. Contributions to Mineralogy and Petrology 98, 455–489.
Hodges, K.V., 2000. Tectonics of the Himalaya and southern Tibet from two perspectives. Geological Society of America Bulletin 112, 324–350.
Hoefs, J., 2009. Stable Isotope Geochemistry, 5th ed. Springer-Verlag, Berlin, Heidelberg p. 244.
Hoskin, P.W., Schaltegger, U., 2003. The composition of zircon and igneous and metamorphic petrogenesis. Reviews in Mineralogy and Geochemistry 53, 27–62.
Ickert, R.B., Hiess, J., Williams, I.S., Holden, P., Ireland, T.R., Lanc, P., et al., 2008. Determining high precision, in situ, oxygen isotope ratios with a SHRIMP II: Analyses of MPI-DING silicate-glass reference materials and zircon from contrasting granites. Chemical Geology 257, 114–128.
Jacobsen, S.B., Pimentel-Klose, M.R., 1988. Nd isotopic variations in Precambrian banded iron formations. Geophysical Research Letters 15, 393–396.
Kalsbeek, F., Affaton, P., Ekwueme, B., Freid, R., Thranea, K., 2012. Geochronology of granitoid and metasedimentary rocks from Togo and Benin, West Africa: comparisons with NE Brazil. Precambrian Research 196–197, 218–233.
Kaneko, Y., Katayama, I., Yamamoto, H., Misawa, K., Ishikawa, M., Rehman, H.U., Shiraishi, K., 2003. Timing of Himalayan ultrahigh-pressure metamorphism: sinking rate and subduction angle of the Indian continental crust beneath Asia. Journal of Metamorphic Geology 21, 589–599.
Kenah, C., Hollister, L.S., 1983. Anatexis in the Central Gneiss Complex, British Columbia. In: Atherton, M.P., Grimbbe, C.D. (Eds.), Migmatites, Melting and Metamorphism. Shiva, Nantwich, U.K., pp. 142–162.
Klein, E.L., Moura, C.A.V., 2008. São Luís Craton and Gurupi Belt (Brazil): Possible Links with the West African Craton and Surrounding Pan-African Belts. In: Pankhurst, R.J., Trouw, R.A.J., Brito Neves, B.B., De Wit, M.J. (Eds.), West Gondwana: Pre-Cenozoic Correlations Across the Atlantic Region, Geological Society, London, Special Publications 294, 137–151.
Klootwijk, C.T., Gee, J.S., Peirce, J.W., Smith, G.M., McFadden, P.L., 1992. An early India-Asia contact: paleomagnetic constraints from Ninetyeast Ridge, ODP leg 121. Geology 20, 395–398.
Lapierre, H., Bendali, M., Dupont, P.L., Gravelle, M., 1986. Nouvelles donnees stratigraphiques et structurales sur le rameau oriental de la chaıne pharusienne, region de Silet (Hoggar, Algerie). Comptes Rendus de l'Academie des Sciences Paris 303, 1731–1736.
Laux, J.H., Pimentel, M.M., Dantas, E.L., Armstrong, R., Junges, S.L., 2005. Two Neo-proterozoic crustal accretion events in the Brasília Belt, central Brazil. Journal of South American Earth Sciences 18, 183–198.
Lee, C.T.A., Morton, D.M., Kistler, R.W., Baird, A.K., 2007. Petrology and tectonics of Phanerozoic continent formation: from island arcs to accretion and continental arc magmatism. Earth and Planetary Science Letters 263, 370–387.
Leech, L.L., 2001. Arrested orogenic development: eclogitization, delamination, and tectonic collapse. Earth and Planetary Science Letters 185, 149–159.
Leech, M.L., Singh, S., Jain, A.K., Klemperer, S.L., Manickavasagam, R.M., 2005. The onset of India-Asia continental collision: early, steep subduction required by the timing of UHP metamorphism in the western Himalaya. Earth and Planetary Science Letters 234, 83–97.
Liégeois, J.P., Bertrand, J.M., Black, R., 1987. The subduction-and collision-related Pan-African composite batholith of the Adrar des Iforas (Mali): A review. Geological Journal 22, 185–211.
Liou, J.G., Tsujimori, T., Zhang, R.Y., Katayama, I., Maruyama, S., 2004. Global UHP metamorphism and continental subduction/collision: the Himalayan model. International Geology Review 46, 1–27.
Liu, Y., Zong, K., Kelemen, P.B., Gao, S., 2008. Geochemistry and magmatic history of eclogites and ultramafic rocks from the Chinese continental scientific drill hole: subduction and ultrahigh-pressure metamorphism of lower crustal cumulates. Chemical Geology 247, 133–153.
Ludwig, K.R., 2001. Squid 1.02 — A User's Manual. Berkeley Geochronology Center. Special, Publication No 2.
Ludwig, K.R., 2003. Isoplot 3.00 — A Geochronological Toolkit for Microsoft Excel. Berkeley Geochronology Center. Special, Publication No 4.
Martin, H., Smithies, R.H., Rapp, R., Moyen, J.F., Champion, D., 2005. An overview of adakite, tonalite–trondhjemite–granodiorite (TTG), and sanukitoid: relationships and some implications for crustal evolution. Lithos 79, 1–24.
Martins, G., Oliveira, E.P., Lafon, J.M., 2009. The Algodões amphiboliteetonalite gneiss sequence, Borborema Province, NE Brazil: geochemical and geochrono-logical evidence for Palaeoproterozoic accretion of oceanic plateau/back-arc basalts and adakitic plutons. Gondwana Research 15, 71–85.
Matteini, M., Junges, S.L., Dantas, E.L., Pimentel, M.M., Bühn, B., 2010. In situ zircon U-Pb and Lu-Hf isotope systematic on magmatic rocks: insights on the crustal evolution of the Neoproterozoic Goiás Magmatic Arc, Brasília belt, Central Brazil. Gondwana Research 17, 1–12.
McDonough, W.F., Sun, S.S., 1995. The composition of the earth. Chemical Geology 120, 223–254.
McMillan, N.J., Harmon, R.S., Moorbath, S., Lopez-Escobar, L., Strong, D.F., 1989. Crustal sources involved in continental arc magmatism: a case study of volcan Mocho-Choshuenco, southern Chile. Geology 17, 1152–1156.
Neves, S.P., 2003. Proterozoic history of the Borborema Province (NE Brazil): correlations with neighboring cratons and Pan-African belts, and implications for the evolution of western Gondwana. Tectonics 22, 1031.
Oliveira, E.P., Windley, B.F., Araujo, M.N.C., 2010. The Neoproterozoic Sergipano orogenic belt, NE Brazil: a complete plate tectonic cycle in western Gondwana. Precambrian Research 181, 64–84.
Padilha, A.L., Vitorello, Í., Pádua, M.B., Bologna, M.S., 2014. Electromagnetic constraints for subduction zones beneath the northwest Borborema province: Evidence for Neoproterozoic island arc-continent collision in northeast Brazil. Geology 42, 91–94.
Pearce, J.A., Harris, N.B.W., Tindle, A.W., 1984. Trace element discrimination diagrams for the tectonic interpretation of granitic rocks. Journal of Petrology 25, 956–983.
Peccerillo, A., Taylor, S.R., 1976. Geochemistry of Eoceno calc-alkaline volcanic rocks from the Kastamonu area, northern Turkey. Contributions to Mineralogy and Petrology 58, 63–81.
Petterson, M.G., 2010. A review of the geology and tectonics of the Kohistan island arc, north Pakistan. Geological Society, London, Special Publications 338, 287–327.
Pimentel, M.M., Fuck, R.A., 1992. Neoproterozoic crustal accretion in central Brazil. Geology 20, 375–379.

Pimentel, M.M., Fuck, R.A., Botelho, N.F., 1999. Granites and the geodynamic history of the Neoproterozoic Brasılia belt, central Brazil: a review. Lithos 46, 463–483.
Pimentel, M.M., Fuck, R.A., Jost, H., Ferreira Filho, C.F., Araujo, S., 2000. The Basement of the Brasília Fold Belt and the Goiás Magmatic Arc. In: Cordani, U.G., Milani, E.J., Thomaz Filho, A., Campos, D.A. (Eds.), Tectonic Evolution of South America. Rio de Janeiro, pp. 151–182.
Santos, T.J.S., Dantas, E.L., Fuck, R.A., Rosa, F.F.da, GanadedeAraujo, C.E., Amaral, W.S., 2007. The Geology and U-Pb and Sm-Nd Geochronology From the Northern Portion of the Santa Quitéria Batholith, NE Brazil. Simpósio Nacional de estudos Tectônicos, 2007. Miut45 3Natal-RN, Anais, pp. 142–144.
Santos, T.J.S., Garcia, M.G.M., Amaral, W.S., Wernick, E., Dantas, E.L., Arthaud, M.H., Caby, R., Santosh, M., 2009. Relics of eclogite facies assemblages in the Ceará Central Domain, NW Borborema Province, NE Brazil: implications for the assembly of West Gondwana. Gondwana Research 15, 454–470.
Santos, T.J.S., Amaral, W.S., Ancelmi, M.F., Dantas, E.L., Fuck, R.A., Pitarello, M.Z., 2013. A Faixa Eclogítica de Forquilha e Sua Importância no Contexto Tectônico da Província Borborema. 25th Simpósio de Geologia do Nordeste, Recife, Brazil, p. 525.
Sato, K., Tassinari, C.C.G., Kawashita, K., Petronilho, L., 1995. O método geocronológico Sm-Nd no IG/USP e suas aplicações. Anais da Academia Brasileira de Ciências 67, 315–336.
Sato, K., Siga Jr., O., Silva, J.A., McReath, I., Liu, D., Iizuka, T., Rino, S., Hirata, T., Sproesser, W. M., Basei, M.A.S., 2009. In situ isotopic analyses of U and Pb in Zircon by remotely operated SHRIMP II, and Hf by LA-ICP-MS: an example of dating and genetic evolution of zircon by 176Hf/177Hf from the Ita Quarry in the Atuba Complex, SE Brazil. Geologia USP, Série Cientifica São Paulo 9, 61–69.
Sawyer, E.W., 1998. Formation and evolution of granite magmas during crustal reworking: the significance of diatexites. Journal of Petrology 39, 1147–1167.
Sawyer, E.W., 2008. Atlas of Migmatites. The Canadian Mineralogist. Special Publication, vol. 9. NRC Research Press, Ottawa, Ontario, p. 371.
Schaltegger, U., Zeilinger, G., Frank, M., Burg, J.P., 2002. Multiple mantle sources during island arc magmatism: U-Pb and Hf isotopic evidence from the Kohistan arc complex, Pakistan. Terra Nova 14, 461–468.
Schandl, E.S., Gorton, M.P., 2002. Application of high field strength elements to discriminate tectonic settings in VMS environments. Economic Geology 97, 629–642.
Scherer, E.E., Whitehouse, M.J., Münker, C., 2007. Zircon as a monitor of crustal growth. Elements 3, 19–24.
Shand, S.J., 1947. Eruptive Rocks, their Genesis, Composition, Classification, and their Relation to Ore-deposits, third ed. John Wiley and Sons, New York 488 pp.
Söderlund, U., Patchett, J.P., Vervoort, J.D., Isachsen, C.E., 2004. The 176Lu decay constant determined by Lu-Hf and U-Pb isotope systematics of Precambrian mafic intrusions. Earth and Planetary Science Letters 219, 311–324.
Stacey, J.S., Kramer, J.D., 1975. Approximation of terrestrial lead isotope by a two-stage model. Earth and Planetary Science Letters 26, 207–212.
Sun, S.S., McDonough, W.F., 1989. Chemical and isotopic systematics of oceanic basalts: implication for manle composition and processes. In: Saunders, A.D., Norry, M.J. (Eds.), Magmatism in Ocean Basins. Geological Society, London, Special Publications 42, 313–345.
Tatsumi, Y., 1986. Formation of the volcanic front in subduction zones. Geophysical Research Letters 13, 717–720.
Tatsumi, Y., 2005. The subduction factory: how it operates in the evolving Earth. GSA Today 15, 4.
Tatsumi, Y., Eggins, S., 1995. Subduction Zone Magmatism. Blackwell Science, Oxford.
Tatsumi, Y., Kogiso, T., 2003. The subduction factory: its role in the evolution of the Earth's crust and mantle. Geological Society, London, Special Publications 219, 55–80.
Treloar, P.J., Petterson, M.G., Jan, M.Q., Sullivan, M.A., 1996. A re-evaluation of the stratigraphy and evolution of the Kohistan arc sequence, Pakistan Himalaya: implications for magmatic and tectonic arc-building processes. Journal of the Geological Society 153, 681–693.
Van Schmus, W.R., Oliveira, E.P., Da Silva Filho, A., Toteu, S.F., Penaye, J., Guimarães, I.P., 2008. Proterozoic links between the Borborema Province, NE Brazil, and the Central African Fold Belt. In: Pankhurst, R.J., Trouw, R.A.J., Brito Neves, B.B., De Wit, M.J. (Eds.), West Gondwana: Pre-Cenozoic Correlations Across the Atlantic Region, Geological Society, London, Special Publications 294, 69–99.
Vervoort, J.D., Patchett, P.J., Blichert-Toft, J., Albarede, F., 1999. Relationship between Lu-Hf and Sm-Nd isotopic systems in the global sedimentary system. Earth and Planetary Science Letters 168, 79–99.
Weinberg, R.F., Dunlap, W.J., 2000. Growth and deformation of the Ladakh Batholith, northwest Himalayas: implications for timing of continental collision and origin of calc-alkaline batholiths. The Journal of Geology 108, 303–320.
Weinberg, R.F., Hasalova, P. (submitted). Water-fluxed melting of the continental crust: a review. Lithos.
White, R.W., Pomroy, N.E., Powell, R., 2005. An in situ metatexite-diatexite transition in upper amphibolite facies rocks from Broken Hill, Australia. Journal of Metamorphic Geology 23, 579–602.
Williams, I.S., 1998. In: McKibben, M.A., Shanks, W.C., Ridley, W.I. (Eds.), U-Th-Pb geochronology by ion microprobe, applications of microanalytical techniques to understanding mineralizing processesReviews in Economic Geology 7, 1–35.
Wu, R.X., Zheng, Y.F., Wu, Y.B., Zhao, Z.F., Zhang, S.B., Liu, X., Wu, F.Y., 2006. Reworking of juvenile crust: element and isotope evidence from Neoproterozoic granodiorite in South China. Precambrian Research 146, 179–212.
Yamamoto, S., Senshu, H., Rino, S., Omori, S., Maruyama, S., 2009. Granite subduction: arc subduction, tectonic erosion and sediment subduction. Gondwana Research 15, 443–453.
Zincone, S.A., 2011. Petrogênese do Batólito Santa Quitéria: Implicações ao Magmatismo Brasiliano na Porção Norte da Província Borborema, NE Brasil. (Master dissertation) Universidade Estadual de Campinas (160 pp.).